WOLFRAM SYNDROME

Activation of the sigma-1 receptor chaperone alleviates symptoms of Wolfram syndrome in preclinical models

Lucie Crouzier[1]†, Alberto Danese[2]†, Yuko Yasui[3], Elodie M. Richard[1], Jean-Charles Liévens[1], Simone Patergnani[2], Simon Couly[1,3], Camille Diez[1], Morgane Denus[1], Nicolas Cubedo[1], Mireille Rossel[1], Marc Thiry[4], Tsung-Ping Su[3], Paolo Pinton[2], Tangui Maurice[1], Benjamin Delprat[1]*

The Wolfram syndrome is a rare autosomal recessive disease affecting many organs with life-threatening consequences; currently, no treatment is available. The disease is caused by mutations in the *WSF1* gene, coding for the protein wolframin, an endoplasmic reticulum (ER) transmembrane protein involved in contacts between ER and mitochondria termed as mitochondria-associated ER membranes (MAMs). Inherited mutations usually reduce the protein's stability, altering its homeostasis and ultimately reducing ER to mitochondria calcium ion transfer, leading to mitochondrial dysfunction and cell death. In this study, we found that activation of the sigma-1 receptor (S1R), an ER-resident protein involved in calcium ion transfer, could counteract the functional alterations of MAMs due to wolframin deficiency. The S1R agonist PRE-084 restored calcium ion transfer and mitochondrial respiration in vitro, corrected the associated increased autophagy and mitophagy, and was able to alleviate the behavioral symptoms observed in zebrafish and mouse models of the disease. Our findings provide a potential therapeutic strategy for treating Wolfram syndrome by efficiently boosting MAM function using the ligand-operated S1R chaperone. Moreover, such strategy might also be relevant for other degenerative and mitochondrial diseases involving MAM dysfunction.

INTRODUCTION

The Wolfram syndrome (WS; OMIM #598500) is an extremely severe rare neurodegenerative disease affecting 1/100,000 to 1/700,000 people worldwide (*1*). The pathology (*2*) is characterized by diabetes insipidus (DI), diabetes mellitus (DM), optic atrophy (OA), and deafness (*3*). DM is present in 97% of the patients and OA in 98.5% (*4*). Deafness and DI are present in 46 and 29% of the patients, respectively (*4*). Other symptoms could include urinary disorders, pons atrophy, ataxia (*4*, *5*), and psychiatric disorders, including bipolar disorder (*6*), schizophrenia (*7*), suicide (*8*), or mania (*9*). To date, no treatment is available, and most of the affected patients die prematurely. Therefore, there is an urgent need for effective treatments.

WS is due to mutations in *WFS1*. The gene *WFS1* encodes Wolframin, a transmembrane protein of the endoplasmic reticulum (ER) (*10*, *11*). In mice, Wolframin is predominantly expressed in spiral ganglion neurons and cochlear inner hair cells (*12*), retinal ganglion cells (*13*), and β cells of Langerhans islets (*14*). Wolframin is also found ubiquitously including in many parts of the brain and spinal cord (*15*). Wolframin plays a prominent role in Ca^{2+} homeostasis because it could function as or activate an ER Ca^{2+} channel (*16*) and modulate ER stress (*14*). We demonstrated recently that WFS1 deficiency leads to an alteration of the communication between ER and mitochondria within the suborganelles called mitochondria-associated ER membranes (MAMs), triggering mitochondria dysfunction (*17*). MAMs play a role in numerous cellular functions such as calcium transfer, lipid metabolism, autophagy, metabolic control, proteostasis/ER stress, organelle dynamics, and apoptosis (*18*, *19*). Increasing evidence suggests that MAM dysfunction contributes to neurodegenerative processes in WS (*18*, *20*) and in neurodegenerative pathologies, including Alzheimer's, Huntington's, or Parkinson's disease and amyotrophic lateral sclerosis (*21*) as well as metabolic diseases, diabetes (*22*, *23*), or cardiovascular diseases (*24*).

WFS1 deficiency altered proper functioning of the nervous system. On a neuroanatomical view, patients with WS showed a deficit in axon myelination (*25*), suggesting that ER stress–related dysfunction may interact with myelin development or promote myelin degeneration during the progression of WS. Moreover, different groups reported impairments of memory (*25*–*27*) and smell and sleep abnormalities with relatively preserved cognitive performance and psychological health (*28*). In addition, in a large cohort of patients with WS, 32% of the individuals developed cognitive disabilities (*4*), underlining the importance of addressing this critical issue.

We previously reported that in the absence of WFS1, the expression of the neuronal calcium sensor 1 (NCS1) protein is reduced in MAMs by 50%, and this reduction is responsible for a deficit in Ca^{2+} homeostasis and mitochondrial dysfunction (*17*). Overexpression of NCS1 up to physiological value restored cellular deficits (*17*). This experiment demonstrated the possibility to counteract mitochondrial dysfunction by targeting a key protein of the MAMs. Because the MAM proteome offers some redundancy in chaperones and protein partners, boosting the activity of several other key proteins of the MAMs may offer the possibility to restore MAM deficit. One of these candidate proteins is the sigma-1 receptor (S1R). S1R is a highly conserved transmembrane protein highly enriched in MAMs, where it interacts with several partners involved in ER-mitochondria Ca^{2+} transfer and/or activation of the ER stress pathways (*29*, *30*). By stabilizing the conformation of inositol 1,4,5-trisphosphate receptor type 3 (IP_3R3), S1R enhances Ca^{2+} efflux from the ER into the mitochondria (*31*). S1R can be activated/inactivated

[1]MMDN, Univ Montpellier, EPHE, INSERM, Montpellier, France. [2]Department of Medical Sciences, Laboratory for Technologies of Advanced Therapies (LTTA), University of Ferrara, 44121 Ferrara, Italy. [3]Cellular Pathobiology Section, Integrative Neuroscience Research Branch, Intramural Research Program, National Institute on Drug Abuse, NIH, 333 Cassell Drive, Baltimore, MD 21224, USA. [4]Laboratoire de Biologie Cellulaire, Université de Liège, GIGA-Neurosciences, Quartier Hopital, Avenue Hippocrate 15, 4000 Liege 1, Belgium.
*Corresponding author. Email: benjamin.delprat@inserm.fr
†These authors contributed equally to this work.

by small molecules, and accumulating preclinical data suggest that S1R agonists are protectants in neurodegenerative diseases [for review, see (*32*)]. We particularly identified the neuroprotective activity of blarcamesine in preclinical models of Alzheimer's disease, and the drug is now entering phase 3 clinical trial (*33*–*36*). Thus, S1R represented an attractive target to correct MAM dysfunction under neurodegenerative condition. However, the potential efficacy of targeting S1R in MAM dysfunction of genetic origin, as observed in WS, remains to be investigated.

Here, we found that transgenic mouse and zebrafish models of WS show marked behavioral pathological symptoms and that activating S1R, using the prototypic S1R agonist PRE-084 (*37*–*39*), or by overexpressing S1R alleviated the symptoms in vivo and corrected Ca^{2+}-impaired homeostasis and mitochondrial deficits in vitro. The S1R agonist acted as an enhancer of Ca^{2+} transfer from the ER to the cytosol or mitochondria and as a booster of mitochondrial physiology. The drug was able to revert most of the locomotor, cognitive, and mood alterations in mouse and zebrafish models of the disease. Together, our findings revealed that S1R is a promising target for treating WS and that a functional recovery of MAM alterations can be achieved using a pharmacological approach.

RESULTS

Behavioral phenotyping of Wfs1$^{\Delta Exon8}$ mice revealed neurological alterations

General exploration

We first considered the mouse model of WS with complete knockout (KO) of exon 8 in the *Wfs* gene, the *Wfs1*$^{\Delta Exon8}$ line (*40*). This resulted in the deletion of amino acids 360 to 890 in the Wfs1 protein and the fusion between Wfs1 residues 1 to 360 and LacZ. To date, more than 170 mutations have been identified in *WFS1* (*41*) with all types of mutations present (nonsense, missense, and frameshift). The deletion of murine exon 8 should be similar to the human mutation Q366X (*41*, *42*). To assess whether *Wfs1* mutation leads to functional brain defects, we investigated the general mobility of *Wfs1*$^{\Delta Exon8}$ mice using an open-field paradigm, in a circular arena (Fig. 1). Both female and male *Wfs1*$^{\Delta Exon8}$ mice showed reduced locomotion (Fig. 1A) that appeared at most time points examined, with statistically significant differences between *Wfs1*^{WT} and *Wfs1*$^{\Delta Exon8}$ females ($P = 0.0133$ at time point 4, $P = 0.0256$ at time point 6, and $P = 0.0209$ at time point 10; Fig. 1B) and males ($P = 0.0337$ at time point 6, $P = 0.0047$ at time point 8, and $P = 0.0051$ at time point 10; Fig. 1C). The reduced locomotion resulted from a significant increase in immobility duration ($P = 0.0038$ for females and $P = 0.0340$ for males; Fig. 1D) but not from a decrease in walking speed (Fig. 1E). *Wfs1*$^{\Delta Exon8}$ mice were therefore less active than *Wfs1*^{WT}. Moreover, male but not female *Wfs1*$^{\Delta Exon8}$ mice showed a decreased presence in the center of the arena ($P = 0.0306$; Fig. 1F) that suggested an increased anxiety response as compared to *Wfs1*^{WT}. No difference in latencies to start locomotion at the beginning of the session for both genders (Fig. 1G) was noted; however, there was a gender-specific effect on the numbers of rearings (decreased in females $P = 0.0295$; Fig. 1H) and groomings (decreased in males $P = 0.0014$; Fig. 1I) in *Wfs1*$^{\Delta Exon8}$ mice.

Open-field parameters were also analyzed during the first habituation session of the novel object test in the squared 50 cm–by–50 cm arena (fig. S1). The analysis confirmed a hypolocomotor response

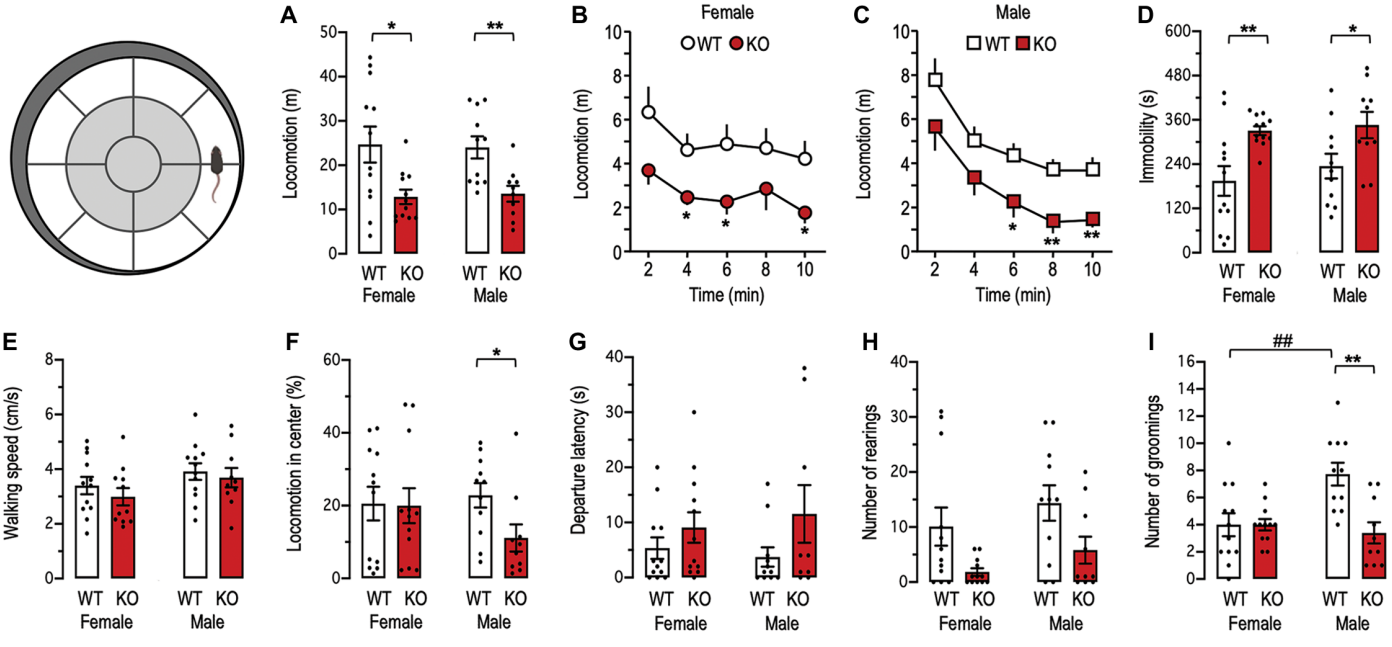

Fig. 1. *Wfs1*$^{\Delta Exon8}$ mice showed hypomobility in the circular open-field test. Female and male *Wfs1*^{WT} (WT) and *Wfs1*$^{\Delta Exon8}$ (KO) animals were placed in the circular open field, and their behaviors were analyzed during 10 min: total locomotion (**A**) and time course for female (**B**) and male mice (**C**), immobility (**D**), walking speed (**E**), locomotion in the center (**F**), departure latency (**G**), and number of rearings (**H**) and groomings (**I**). $n = 10$ to 12 per group. Two-way ANOVAs: $P > 0.05$ for gender, $P < 0.001$ for genotype, and $P > 0.05$ for the interaction in (A); $P > 0.05$ for gender, $P < 0.001$ for genotype, and $P > 0.05$ for the interaction in (D); $P < 0.05$ for gender, $P > 0.05$ for genotype, and $P > 0.05$ for the interaction in (E); $P > 0.05$ for gender, $P < 0.05$ for genotype, and $P > 0.05$ for the interaction in (F); $P > 0.05$ for gender, $P > 0.05$ for genotype, and $P > 0.05$ for the interaction in (G); $P > 0.05$ for gender, $P < 0.05$ for genotype, and $P > 0.05$ for the interaction in (H); $P < 0.05$ for gender, $P < 0.01$ for genotype, and $P < 0.01$ for the interaction in (I). *$P < 0.05$ and **$P < 0.01$ versus WT mice; ##$P < 0.01$ versus female mice; Newman-Keuls test.

in female *Wfs1*$^{\Delta Exon8}$ mice, with a statistically significant decrease in locomotion (P = 0.0224; fig. S1A), increase in immobility (P = 0.0291; fig. S1D), and decrease in walking speed (P = 0.0477; fig. S1E), as compared to *Wfs1*^{WT} animals. The percentage of presence in the center of the arena was significantly decreased for female (P = 0.0002) but not male (P = 0.2107) *Wfs1*$^{\Delta Exon8}$ animals (fig. S1F). Different outcomes were therefore observed depending on the open-field paradigm (circular versus squared arena), but they convergently showed that *Wfs1*$^{\Delta Exon8}$ mice presented reduced locomotion and signs of increased anxiety.

Learning and memory

The learning and memory abilities of *Wfs1*$^{\Delta Exon8}$ mice were examined using complementary tests assessing spatial working memory (spontaneous alternation), recognition memory (novel object test), long-term contextual memory (passive avoidance), and spatial reference memory (place learning in the water maze). Both female and male *Wfs1*$^{\Delta Exon8}$ mice showed marked spontaneous alternation deficits when exploring the Y-maze (Fig. 2A). *Wfs1*$^{\Delta Exon8}$ mice explored the maze less during the session (Fig. 2B), a coherent observation with the reduced locomotion previously noted. In the novel object test, only mice interacting with both objects were included in the study. Animals performed 10 to 17 contacts with objects in session 2 (presenting two similar objects) and 17 to 28 in session 3 (presenting a familiar and a novel object), with no difference among groups. In session 2, animals showed a similar interaction with the two objects (Fig. 2C). In session 3, both *Wfs1*^{WT} and *Wfs1*$^{\Delta Exon8}$ female mice explored significantly more the novel object than the familiar one [P = 0.0074 versus 50% for wild type (WT) and P = 0.0327 for KO; Fig. 2D]. However, only male *Wfs1*^{WT} mice but not male *Wfs1*$^{\Delta Exon8}$ mice showed a preferential exploration of the novel object (P = 0.0061 for WT and P = 0.9663 for KO; Fig. 2D). In the passive avoidance test, both female and male *Wfs1*$^{\Delta Exon8}$ mice did not show differences in the latency to enter the dark compartment during the training session (Fig. 2E). Male, but not female, *Wfs1*$^{\Delta Exon8}$ mice showed a moderate, but significant (P = 0.0367), decrease in step-through latency during the retention test (Fig. 2F) and a significant increase in escape latency (P = 0.0007; Fig. 2G), demonstrating that male *Wfs1*$^{\Delta Exon8}$ mice present a deficit in long-term contextual memory. In the water maze test, all groups showed decreased swim duration to reach the platform location after training sessions; however, *Wfs1*$^{\Delta Exon8}$ mice appeared less effective than *Wfs1*^{WT}. Female *Wfs1*$^{\Delta Exon8}$ mice showed higher latencies than *Wfs1*^{WT} during the three last trials (P = 0.0277 for swim trial 4 and P = 0.0392 for swim trial 5; Fig. 2H). No difference was noted in male *Wfs1*$^{\Delta Exon8}$ mice compared to controls (Fig. 2I). Moreover, both female and male *Wfs1*$^{\Delta Exon8}$ mice showed statistically significant decreases in the acquisition slope calculated over the five training trials (P = 0.0197 for females and P = 0.0085 for males; Fig. 2J), confirming their weaker training performance. Both female and male *Wfs1*$^{\Delta Exon8}$ mice swam slightly but significantly less rapidly than *Wfs1*^{WT} animals (P = 0.0028 for females and P = 0.0185 for males; Fig. 2K). Analyses of swimming as path lengths instead of swimming duration did not change the acquisition profile analysis. When mice were submitted to the probe test, 48 hours after the last training trial, all groups showed preferential exploration of the training quadrant, as compared to the other quadrants, and the presence was significantly higher than hazard level (P = 0.0037 versus 15 s for female WT, P = 0.0224 for female KO, P = 0.0155 for male WT, and P = 0.0012 for male KO; Fig. 2, L and M). These data showed that mice acquired the spatial information. Last, the platform was moved from the northeast to the southwest quadrant, with a flag placed on it. In this visible platform version, both female (Fig. 2N) and male (Fig. 2O) animals were able to rapidly reach the platform, confirming that visual ability of *Wfs1*$^{\Delta Exon8}$ mice was correct at this age.

Therefore, *Wfs1*$^{\Delta Exon8}$ mice presented memory deficits that were very consistent in males and observable in all the procedures tested. These deficits were particularly marked for spontaneous alternation and novel object tests, evaluating an episodic-like form of recognition memory. The passive avoidance retention parameters that assessed contextual long-term memory were also altered as well as the acquisition of place learning in the water maze.

Anxiety

An alteration of the anxious response of *Wfs1*$^{\Delta Exon8}$ mice was initially suggested by the diminution of presence in the center of the open fields. We analyzed the mice behavior using two classical tests, the black-and-white box exploration (Fig. 3, A to D) and elevated plus maze (Fig. 3, E and H). The number of crossings between the light and dark compartments of the box was similar among groups (Fig. 3B), and both female and male *Wfs1*$^{\Delta Exon8}$ mice did not show differences in the time spent in the light compartment (Fig. 3C). The time per visit in the light compartment was decreased in female (P = 0.0492) but not male (P = 0.2897; Fig. 3D) animals. In the elevated plus maze, the number of arm entries was similar among groups (Fig. 3F), but the time in the open arms (Fig. 3G) and the time per visit (Fig. 3H) were significantly decreased for female *Wfs1*$^{\Delta Exon8}$ mice as compared to *Wfs1*^{WT} controls (P = 0.0150 for the time and P = 0.0335 for the time per visit) but not for male mice. Anxiety-related responses showed, therefore, some alterations in *Wfs1*$^{\Delta Exon8}$ mice, more consistently in female compared to male animals.

Identification of S1R as a potential target for pharmacological intervention in Wfs1$^{\Delta Exon8}$ mice

In fibroblasts from patients with WS, WFS1 mutation resulted in a decreased expression of NCS1 in MAMs and thus in reduced NCS1-induced modulation of IP_3R-gated Ca^{2+} transfer from the ER into the mitochondria (*17*). We measured a statistically significant 20% reduction in the expression of NCS1 in the hippocampus (P = 0.0080; Fig. 4A) and cortex of *Wfs1*$^{\Delta Exon8}$ mice (P = 0.0339; Fig. 4B) and thus confirmed a direct repercussion of WFS1 invalidation on NCS1 protein amounts. Among the numerous regulatory proteins modulating IP_3R activity, we focused on S1R, an ideal candidate for a pharmacological intervention. S1R expression was not affected in the hippocampus (Fig. 4C) or cortex (Fig. 4D) of *Wfs1*$^{\Delta Exon8}$ mice as compared to *Wfs1*^{WT} animals. We also examined NCS1 and WFS1 expression in S1R KO mice (Fig. 4, E and H). NCS1 expression was unchanged in the hippocampus (Fig. 4E) and in the cortex (P = 0.1117; Fig. 4F). WFS1 was unchanged in the hippocampus (Fig. 4G) and cortex (Fig. 4H) of S1R KO mice. We examined in a cellular model, cultured murine Neuro2a cells, whether S1R could interact with WFS1 or NCS1 under physiological conditions. S1R-V5 was overexpressed in Neuro2a cells, and WFS1 or NCS1 was immunoprecipitated (Fig. 4I). The interaction was validated by visualizing the coimmunoprecipitation of S1R-V5. Immunoglobulin G (IgG) immunoprecipitation was used as a negative control. S1R partially coimmunoprecipitated with NCS1 and much more faintly with WFS1 (Fig. 4I), suggesting a direct link between at least S1R and NCS1 proteins. This physical interaction

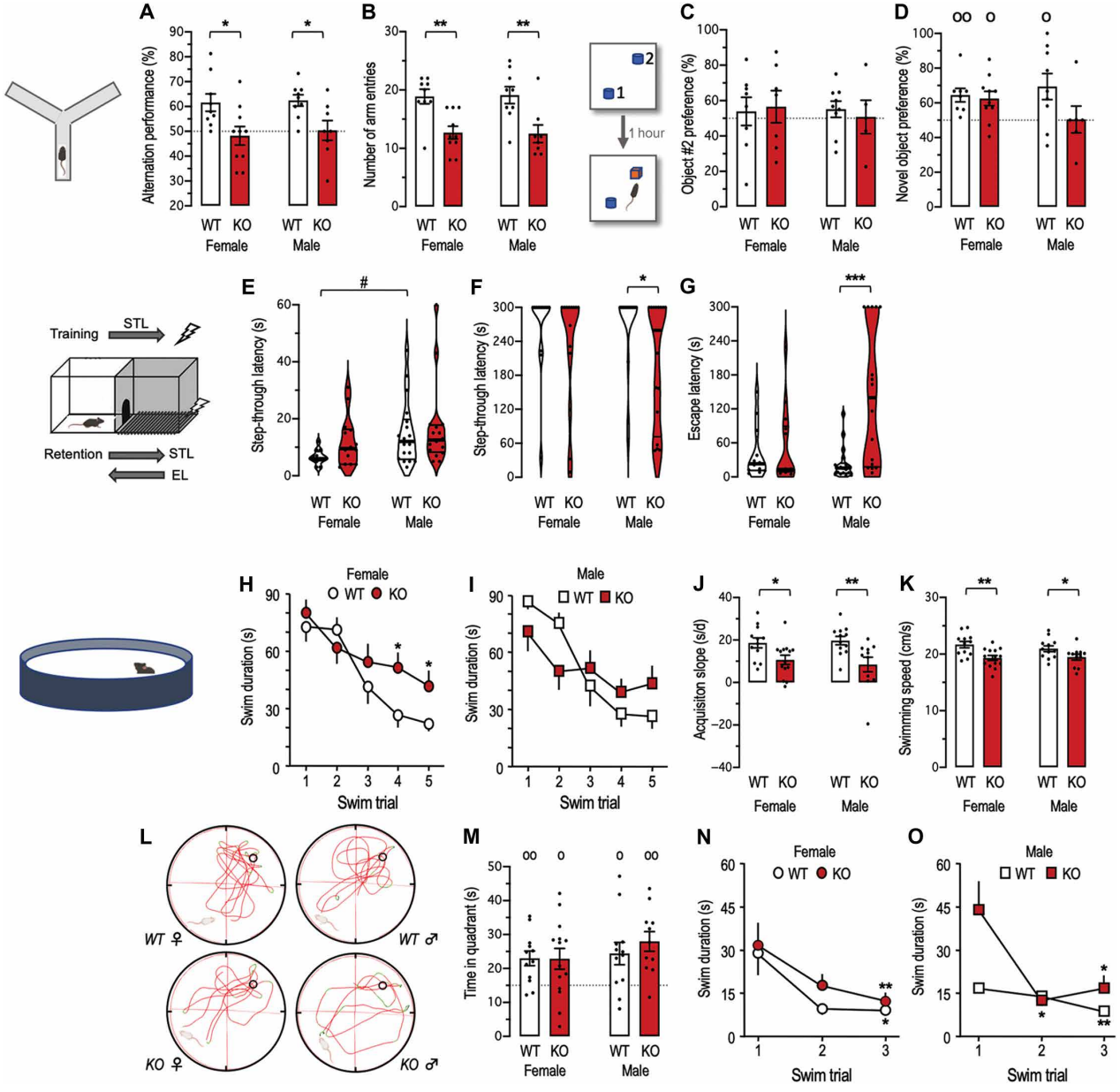

Fig. 2. *Wfs1*$^{\Delta Exon8}$ mice showed learning and memory deficits more pronounced in males. *Wfs1*^{WT} (WT) and *Wfs1*$^{\Delta Exon8}$ (KO) mice were tested for spontaneous alternation in the Y-maze (**A** and **B**), object recognition (**C** and **D**), passive avoidance (**E** to **G**), and place learning in the water maze (**H** to **O**). (A) Spontaneous alternation performance and (B) total number of arm entries during the 8-min session in the Y-maze. (C) Preference for the object in position #2 during session 2 with two identical objects and (D) preference for the novel object in position #2 during session 3 of the object recognition test. (E) Step-through latency (STL) during passive avoidance training and (F) step-through latency and (G) escape latency (EL) during the retention test performed 24 hours after training. Violin graphs show individual data distribution with median and interquartile range. Acquisition profiles of the location of an invisible platform, placed in the northeast quadrant of the pool, for female (H) or male (I) mice. Training during 5 days consisted of three swims per day with 15-min intertrial time interval. (J) Acquisition slopes were calculated from individual acquisition profile. The swimming speed is shown in (K). On day 7, the platform was removed, and mice were submitted to a probe test. Typical paths are shown in (L). The presence in the training quadrant was analyzed (M). On day 8, the platform was moved to the southwest quadrant and rendered visible by placing a flag on it. Acquisition was analyzed with three swims with 15-min intertrial time interval for female (N) and male mice (O). $n = 8$ to 10 per group in (A) and (B), 5 to 9 in (C) and (D), 12 to 18 in (E) to (G), and 11 to 14 in (H) to (O). Two-way ANOVAs: $P > 0.05$ for gender, $P < 0.001$ for genotype, and $P > 0.05$ for the interaction in (A); $P > 0.05$ for gender, $P < 0.0001$ for genotype, and $P > 0.05$ for the interaction in (B); $P > 0.05$ for gender, $P < 0.001$ for genotype, and $P > 0.05$ for the interaction in (J); $P > 0.05$ for gender, $P < 0.001$ for genotype, and $P > 0.05$ for the interaction in (K). Kruskal-Wallis ANOVAs: $P < 0.05$ in (E); $P > 0.05$ in (F); $P < 0.05$ in (G). Friedman nonparametric repeated-measure ANOVAs: $P < 0.0001$; trial 4 versus trial 1: $P < 0.01$, trial 5 versus trial 1: $P < 0.001$ for WT in (H); $P < 0.05$; trial 5 versus trial 1: $P < 0.05$ for KO in (H); $P < 0.0001$; trial 3 versus trial 1: $P < 0.05$, trial 4 versus trial 1: $P < 0.001$, trial 5 versus trial 1: $P < 0.01$ for WT in (I): $P > 0.05$ for KO in (I); $P < 0.05$; trial 3 versus trial 1: $P < 0.05$ for WT in (N); $P < 0.01$; trial 3 versus trial 1: $P < 0.01$ for KO in (N); $P < 0.01$; trial 3 versus trial 1: $P < 0.01$ for WT in (O); $P < 0.01$; trial 2 versus trial 1: $P < 0.05$, trial 3 versus trial 1: $P < 0.05$ for KO in (O). $^{*}P < 0.05$, $^{**}P < 0.01$, and $^{***}P < 0.001$ versus WT mice; $\#P < 0.05$ versus female mice; Newman-Keuls test in (A), (B), (J), and (K); Mann-Whitney test in (E) to (G). $^{\circ}P < 0.05$ and $^{\circ\circ}P < 0.01$ versus 50% level in (C) and (D) or 15-s level in (M), one-sample *t* test.

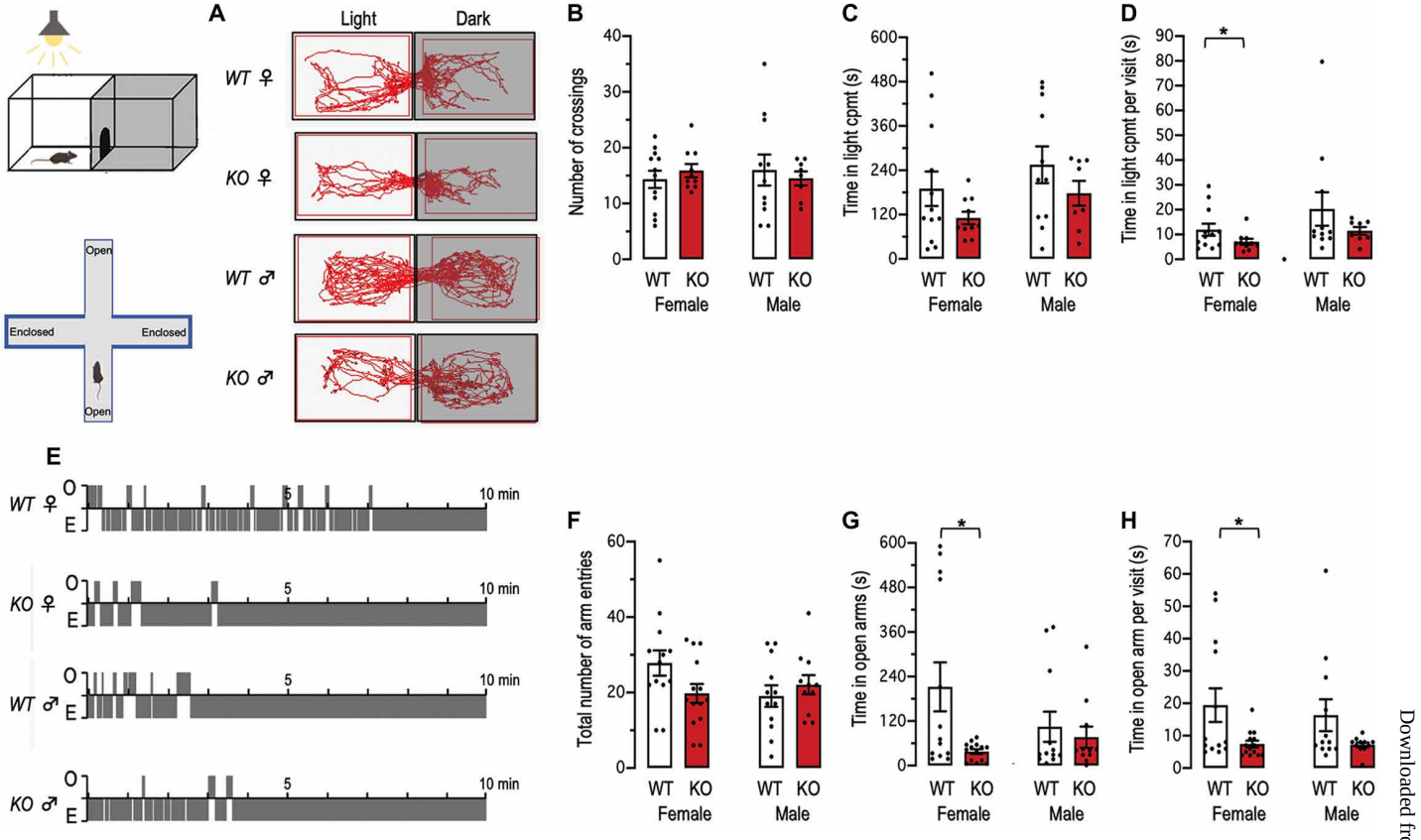

Fig. 3. *Wfs1*$^{\Delta Exon8}$ mice showed increased anxiety particularly in females. *Wfs1*^{WT} (WT) and *Wfs1*$^{\Delta Exon8}$ (KO) mice were tested in the black-and-white exploration box (**A** to **D**) and in the elevated plus maze (**E** to **H**). (A) Typical video-tracked patterns are shown for WT and *Wfs1* KO mice in the black-and-white box. (B) The number of crossings between the light and dark compartments, (C) time in the light compartment, and (D) time per visit in the light compartment. (E) Typical time-course presence in the open (O) or enclosed (E) arms of the elevated plus maze, (F) total number of arm entries, (G) time in the open arms, and (H) time per visit in the open arms. The number of mice per group is indicated in the columns in (A) and (D). $n = 8$ to 12 per group in (A) to (D) and 11 to 14 in (E) to (H). Two-way ANOVAs: $P > 0.05$ for gender, $P > 0.05$ for genotype, and $P > 0.05$ for the interaction in (B); $P > 0.05$ for gender, $P < 0.05$ for genotype, and $P > 0.05$ for the interaction in (C); $P > 0.05$ for gender, $P < 0.05$ for genotype, and $P > 0.05$ for the interaction in (D); $P > 0.05$ for gender, $P > 0.05$ for genotype, and $P > 0.05$ for the interaction in (F); $P > 0.05$ for gender, $P < 0.05$ for genotype, and $P > 0.05$ for the interaction in (G); $P > 0.05$ for gender, $P < 0.05$ for genotype, and $P > 0.05$ for the interaction in (H). *$P < 0.05$ versus WT mice; Newman-Keuls test.

between the proteins suggested a functional relation. Our hypothesis, illustrated in fig. S2, was therefore that activating S1R could help modulate IP_3R. S1R activation could be achieved in vivo by administration of a selective S1R agonist or possibly by S1R overexpression. This activation would then result in a facilitation/restoration of Ca^{2+} transfer into the mitochondria, even under WS condition when NCS1 expression is altered. Moreover, S1R is a particularly interesting target. It must be considered as an intracellular modulatory chaperone protein, thus not requiring an endogenous ligand stricto sensu. However, it still shares some characteristics as a receptor. In particular, it can be targeted using numerous ligands that therefore act as S1R agonists/activators or antagonist [for a recent review, see (*43*)]. We used PRE-084, a reference S1R agonist (*37*, *39*). The drug presents a very high S1R affinity ($K_i = 44$ nM) and a high selectivity toward other targets [median inhibitory concentration (IC_{50}) > 100,000 nM for the phencyclidine binding site, IC_{50} = 55,702 nM for dopamine D_2 receptor, IC_{50} = 13,953 nM for muscarinic acetylcholine receptor, IC_{50} = 18,748 nM for 5-HT_2 receptor, IC_{50} > 100,000 nM for α-adrenergic receptor, and IC_{50} > 200,000 nM for β-adrenergic receptor] (*39*). In addition, the selectivity toward S1R is very high ($\sigma_2/\sigma_1 = 603$) (*44*). Moreover, the drug behavioral effects were fully blocked by selective S1R antagonists (*37*, *45*), S1R antisense oligodeoxynucleotidic probes (*46*), and in *S1R* KO mice (*47*). We therefore tested PRE-084, at its most active dose in vivo (*37*, *47*), on learning abilities in male *Wfs1*$^{\Delta Exon8}$ mice (Fig. 5, A to I). PRE-084–treated *Wfs1*$^{\Delta Exon8}$ mice showed a significant ($P = 0.0039$) recovery of spontaneous alternation (Fig. 5A). In the novel object test, the treatment did not affect object exploration during session 2 (Fig. 5B) but attenuated the deficit of exploration for the novel object in session 3 (Fig. 5C). In the water maze test, a daily injection of vehicle (V) solution failed to change the delay in acquisition observed for *Wfs1*$^{\Delta Exon8}$ mice as compared to *Wfs1*^{WT} controls (Fig. 5D). Statistically significant differences in latencies were measured during swimming trials 3 ($P = 0.0329$), 4 ($P = 0.0006$), and 5 ($P = 0.0166$). The daily injection of PRE-084 prevented this delay and significantly decreased swimming latencies during the last two trials ($P = 0.0105$ each; Fig. 5E). Calculation of the acquisition slopes confirmed that only V-treated *Wfs1*$^{\Delta Exon8}$ mice showed a statistically significant decrease as compared to V-treated *Wfs1*^{WT} mice ($P = 0.0122$) but not PRE-084–treated *Wfs1*$^{\Delta Exon8}$ mice ($P = 0.2519$; Fig. 5F). The probe test showed that all groups preferentially explored the T quadrant, confirming that *Wfs1*$^{\Delta Exon8}$ mice lastly acquired the

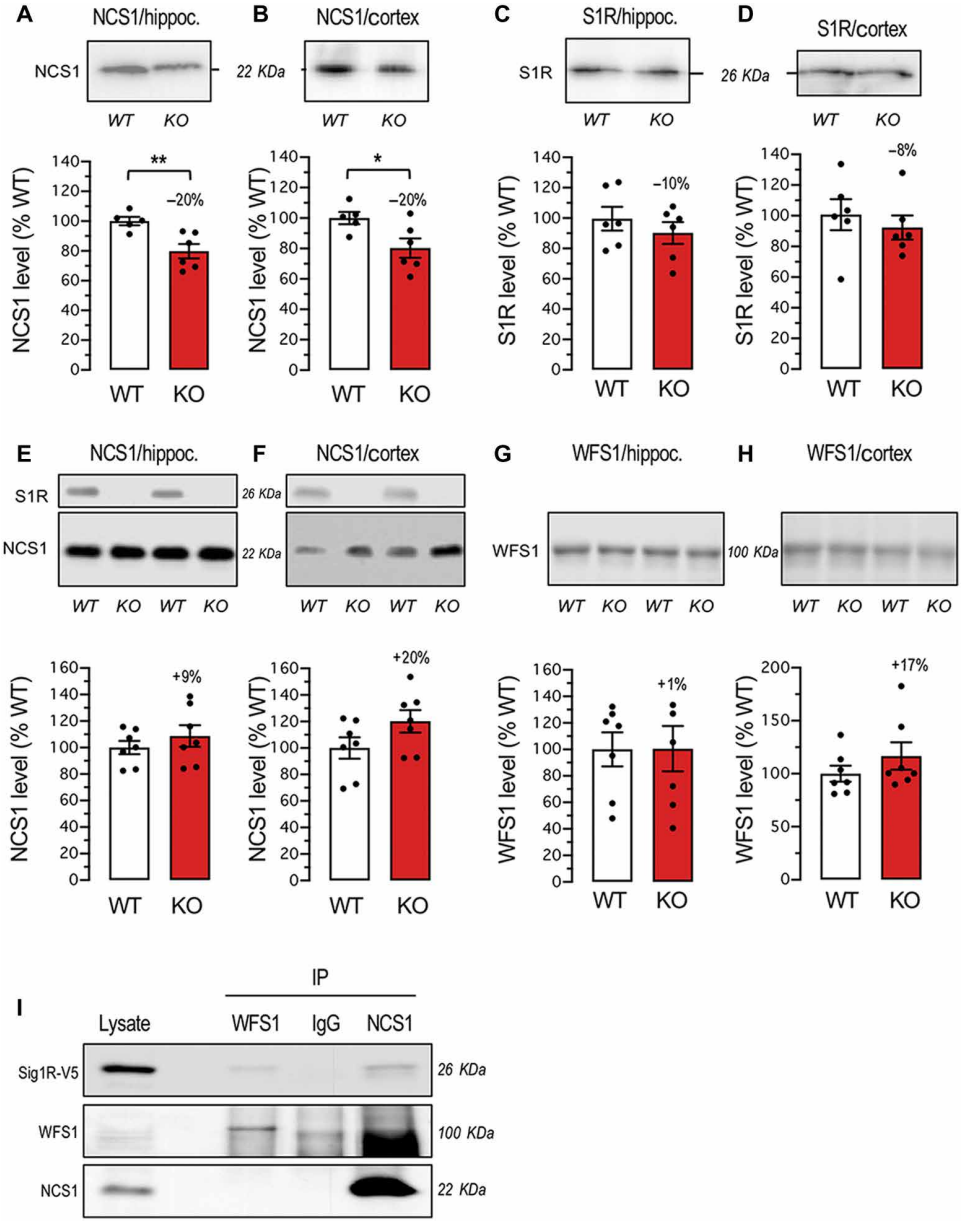

Fig. 4. Expression and interaction analyses of WFS1, NCS1, and S1R. (**A** and **B**) NCS1 and (**C** and **D**) S1R protein amounts in the hippocampus (A and C) and cortex (B and D) of $Wfs1^{WT}$ (WT) and $Wfs1^{\Delta Exon8}$ (KO) mice. (**E** and **F**) NCS1 and (**G** and **H**) WFS1 protein amounts in the hippocampus (E and G) and cortex (F and H) of WT and S1R KO mice. $n = 6$ per group in (A) to (D) and 7 in (E) to (H). $^*P < 0.05$ and $^{**}P < 0.01$ versus WT mice; Newman-Keuls test. (**I**) Coimmunoprecipitation between S1R and WFS1 or NCS1 was examined in WT or SIR-V5 overexpressed Neuro2a cells. Total lysate showed immunoreactivity for WFS1, NCS1, and the S1R-V5. Immunoprecipitation (IP) was performed with WFS1, NCS1, and IgG as a control.

spatial information, and no impact of the PRE-084 was noted (Fig. 5G). During passive avoidance retention, V-treated $Wfs1^{\Delta Exon8}$ mice showed a statistically highly significant deficit ($P = 0.0004$) in step-through latency as compared to V-treated $Wfs1^{WT}$ mice. The PRE-084 treatment did not affect ($P = 0.1172$) the deficit in $Wfs1^{\Delta Exon8}$ mice (Fig. 5H). However, the increase in escape latency measured in $Wfs1^{\Delta Exon8}$ mice, impaired in $Wfs1^{\Delta Exon8}$ mice, was restored ($P = 0.0206$) after PRE-084 treatment (Fig. 5I).

Female $Wfs1^{\Delta Exon8}$ mice were also treated with the S1R agonist and examined in anxiety tests (Fig. 5, J to O). During black-and-white box exploration, PRE-084 treatment resulted in statistically significant effects: The number of crossing was slightly reduced ($P = 0.0175$; Fig. 5J), whereas the time spent in the light compartment ($P = 0.0011$; Fig. 5K) and the time per visit ($P = 0.0003$; Fig. 5L) were increased up to those of $Wfs1^{WT}$ mice. In the elevated plus maze, no impact was noted on maze exploration (Fig. 5M), but the time spent in the open arms was slightly increased, and the PRE-084–treated $Wfs1^{\Delta Exon8}$ mice did not differ ($P = 0.0776$) from V-treated $Wfs1^{WT}$ mice, contrarily to V-treated $Wfs1^{\Delta Exon8}$ mice ($P = 0.0440$; Fig. 5N). The time per visit in the open arms was significantly increased ($P = 0.0173$) after PRE-084 treatment in $Wfs1^{\Delta Exon8}$ mice (Fig. 5O).

Confirmation of the restorative consequence of S1R activity in *wfs1ab*^{KO} zebrafish

The availability of mutant zebrafish lines for the pathology could allow a direct confirmation of the pharmacological relevance on S1R activity of an agonist treatment compared to a direct overexpression of the protein itself. The *wfs1* gene is duplicated in zebrafish, and we used the $wfs1ab^{KO}$ line, generated in the laboratory by crossing $wfs1a^{C799X}$ and $wfs1b^{W493X}$ mutants. These mutations should mimic human mutations E752X or Q819X for $wfs1a^{C799X}$ and Q486X for $wfs1b^{W493X}$ (*41*, *42*). $wfs1ab^{KO}$ zebrafish showed a reduction ($P = 0.0013$) in *wfs1a* mRNA expression but not in *wfs1b* ($P = 0.1744$; Fig. 6A). This was expected because the model was generated by *N*-ethyl-*N*-nitrosourea, leading to a stop codon mutation in *wfs1a* and *wfs1b*, which is not expected to always result in mRNA degradation. mRNA amounts of *sigmar1* and *ncs1*, the latter also duplicated, were not affected in the mutant line (Fig. 6A). Concerning protein detection, antibodies targeting S1R and Ncs1, but not Wfs1, are commercially available and validated in Western blot using KO samples. The analysis of S1R and Ncs1 protein abundance in the zebrafish revealed that they were unaffected (Fig. 6, B and C). Regarding behavioral activity, $wfs1ab^{KO}$ zebrafish showed a clear locomotor alteration when their response to light variation was tested using a visual motor response test (Fig. 6, D to K). Mobility during the light-OFF periods was significantly increased ($P = 0.0020$) in

Fig. 5. The S1R agonist PRE-084 attenuated the deficits of memory in male *Wfs1*$^{\Delta Exon8}$ mice and anxiety in female *Wfs1*$^{\Delta Exon8}$ mice. Vehicle solution (V) or PRE-084 (PRE; 0.3 mg/kg, intraperitoneally) was administered in male *Wfs1*^{WT} (WT) and *Wfs1*$^{\Delta Exon8}$ (KO) mice, 30 min before the Y-maze session (**A**); session 2 in the object recognition test (**B**) with session 3 results shown are in (**C**), or each training day in the water maze test, with data showing acquisition profiles (**D** and **E**) and slope (**F**) and the probe test performed 72 hours after the last training day (**G**), or the training session in the passive avoidance test, with step-through latency for retention shown in (**H**) and escape latency in (**I**). The drug was administered at the same dose in female WT and KO mice, 30 min before the black-and-white exploration box test or the elevated plus maze test. (**J**) The number of crossings between the two compartments, (**K**) duration spent in the light compartment, and (**L**) time per visit for the black-and-white exploration. (**M**) Total number of arm entries, (**N**) time in the open arms, and (**O**) time per visit in the elevated plus maze. $n = 8$ to 12 per group in (A), 6 to 10 in (B) and (C), 12 to 13 in (D) to (G), 10 to 14 in (H) and (I), 9 to 14 in (J) to (L), and 11 to 14 in (M) to (O). Two-way ANOVAs: $P < 0.01$ for treatment, $P < 0.001$ for genotype, and $P < 0.05$ for the interaction in (A); $P < 0.05$ for genotype, $P > 0.05$ for treatment, and $P > 0.05$ for the interaction in (F); $P < 0.05$ for treatment, $P > 0.05$ for genotype, and $P > 0.05$ for the interaction in (J); $P < 0.01$ for treatment, $P > 0.05$ for genotype, and $P < 0.01$ for the interaction in (K); $P < 0.001$ for treatment, $P > 0.05$ for genotype, and $P > 0.05$ for the interaction in (L); $P > 0.05$ for treatment, $P > 0.05$ for genotype, and $P > 0.05$ for the interaction in (M); $P > 0.05$ for treatment, $P < 0.05$ for genotype, and $P > 0.05$ for the interaction in (N); $v > 0.05$ for treatment, $P > 0.05$ for genotype, $F_{(1,47)} = 1.304$, and $P > 0.05$ for the interaction in (O). Kruskal-Wallis ANOVAs: $P < 0.01$ in (H); $P < 0.001$ in (I). Friedman nonparametric repeated-measure ANOVAs: $P < 0.0001$, trials 3 to 5 versus trial 1: $P < 0.001$ for WT/V and $P < 0.05$, trials 2 to 5 versus trial 1: not significant, for KO/V in (D); $P < 0.0001$, trials 3 and 4 versus trial 1: $P < 0.01$; trial 5 versus trial 1: $P < 0.001$ for WT/PRE and $P < 0.0001$, trial 3 versus trial 1: $P < 0.05$, trials 4 and 5 versus trial 1: $P < 0.001$ for KO/PRE in (E). *$P < 0.05$, **$P < 0.01$, and ***$P < 0.001$ versus V-treated WT mice; #$P < 0.05$, ##$P < 0.01$, and ###$P < 0.001$ versus V-treated KO mice; Newman-Keuls test in (A), (C), (D), (F), and (J) to (O); Mann-Whitney test in (H) and (I). °$P < 0.05$, °°$P < 0.01$, and °°°$P < 0.001$ versus 50% level in (C), versus 15-s level in (G); one-sample *t* test.

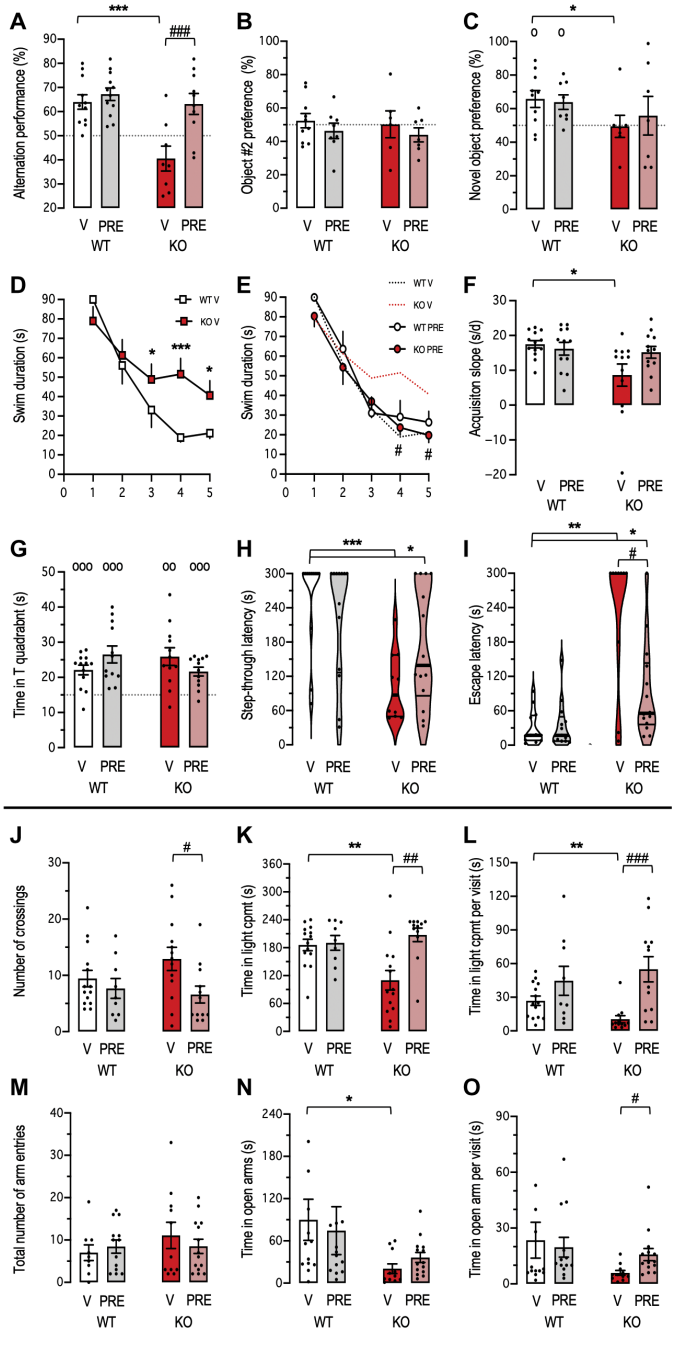

wfs1ab^{KO} larvae as compared to controls (Fig. 6, D and E). The PRE-084 treatment, tested in the 0.1 to 10 μM concentration range in the fish water, resulted in a concentration-dependent decrease in the hyperlocomotor response, down to the mobility of *wfs1ab*^{WT}, at 3 and 10 μM ($P = 0.0065$; Fig. 6, D and E). Cotreatment with the S1R antagonist NE-100 resulted in prevention of the PRE-084 effect, with both drugs being tested at 3 μM (Fig. 6, F and G). When the drug treatments were analyzed by comparing the effect measured in *wfs1ab*^{KO} zebrafish versus *wfs1ab*^{WT} controls, the positive effect of PRE-084 on hypermobility was abolished using NE-100 cotreatment, with the S1R antagonist having no effect alone (Fig. 6H). This observation confirmed the S1R agonist action of PRE-084 in *wfs1ab*^{KO} zebrafish. In a second set of experiments, we transiently overexpressed human S1R by S1R mRNA injection in *wfs1ab*^{KO} line (fig. S3) and compared the mobility response with control fish receiving mCherry control mRNA (Fig. 6, I to K). S1R overexpression in *wfs1ab*^{WT} zebrafish induced a moderate but significant hypermobility response ($P = 0.0262$), and it significantly attenuated ($P = 0.0012$) the hypermobility response observed in mCherry-treated *wfs1ab*^{KO} larvae (Fig. 6, I and J). Analysis of the KO/WT response ratio showed a 74% increase in mCherry-treated controls but only a 12% increase in S1R-overexpressing larvae (Fig. 6K), confirming that increased S1R activity alleviated hypermobility in KO zebrafish.

Functional recovery induced by the S1R agonist in WS is related to MAM physiology in human cells

We previously took advantage of fibroblasts from patients with WS, with WFS1-null mutation, to demonstrate that WFS1 deficiency is associated with decreased mitochondrial Ca^{2+} uptake, decreased ER-mitochondria interactions, and impairments of mitochondrial functionality (*17*). To confirm that the *Wfs1*$^{\Delta Exon8}$ mouse model showed a relevant pathological alteration of MAMs, we determined whether the loss of function of Wfs1 affected the number of contacts between ER and mitochondria by transmission electron microscopy on a hippocampal section (fig. S4, A to C). At first, we observed that

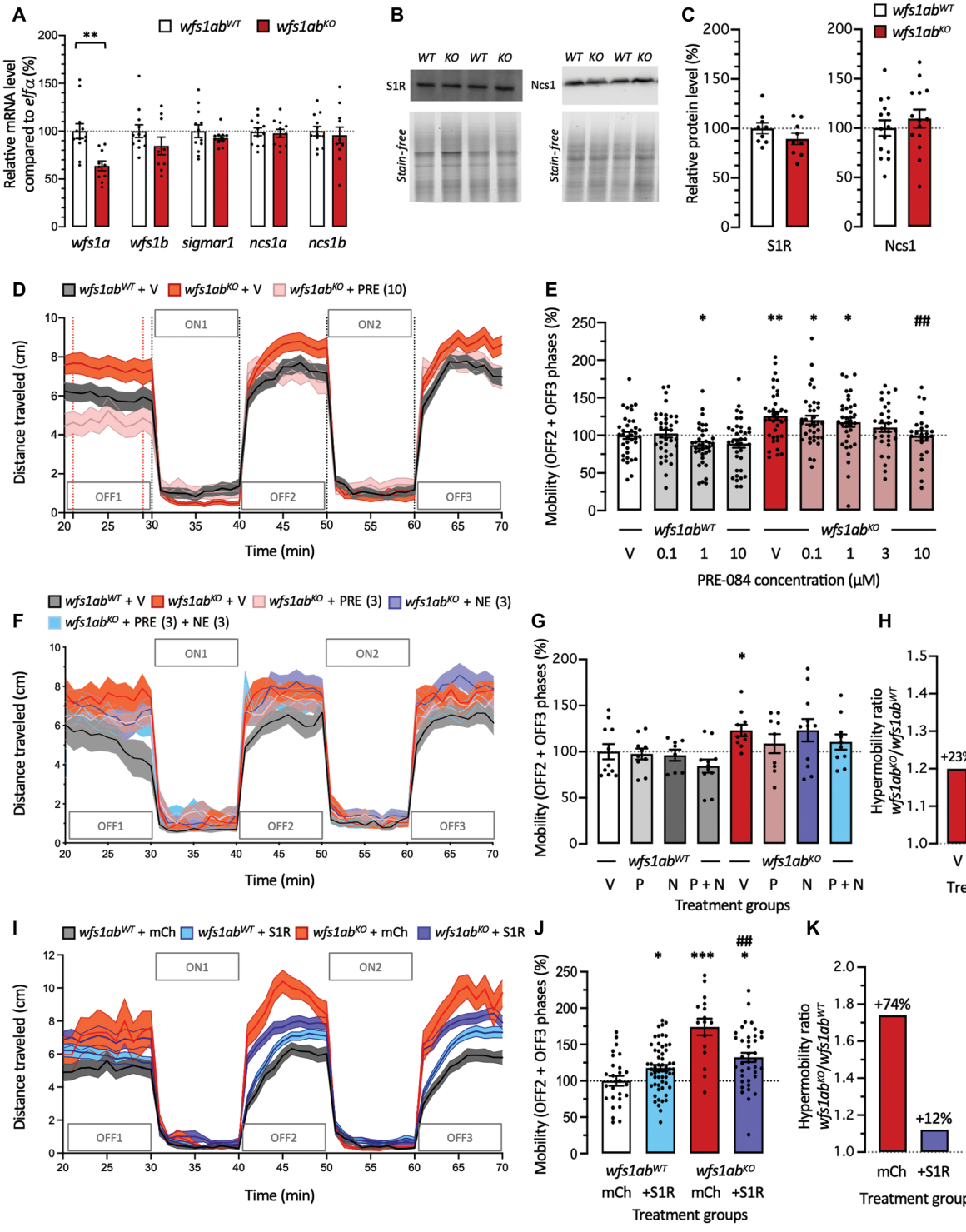

Fig. 6. PRE-084 or overexpression of S1R attenuated the mobility deficits in *wfs1ab*^{KO} zebrafish larvae. (**A**) Quantification of mRNA amounts for *wfs1a*, *wfs1b*, *sigmar1*, *ncs1a*, and *ncs1b* in *wfs1ab*^{WT} and *wfs1ab*^{KO} larvae by RT-PCR. (**B**) Typical blots and (**C**) quantification of protein amounts for S1r and Ncs1. (**D**, **F**, and **I**) Typical mobility patterns in the visual motor response test of zebrafish larvae and (**E**, **G**, and **J**) quantification of cumulated mobility during the OFF2 + OFF3 phases, expressed as percentage of control (V- or mCherry-treated *wfs1*^{WT} larvae). (**H** and **K**) Hypermobility ratio. (D and E) Dose-response effect of PRE-084 (0.1 to 10 µM). (F to H) Blockade of PRE-084 effect by the S1R antagonist NE-100, both drugs being administered at 3 µM. $n = 10$ to 12 per group in (A), 8 to 14 in (B) and (C), 24 to 36 in (D) and (E), 8 to 11 in (F) to (H), and 16 to 58 in (I) to (K). One-way ANOVAs: $P < 0.0001$ in (A); $P < 0.05$ in (G). Two-way ANOVA: $P > 0.05$ for S1R overexpression, $P < 0.0001$ for genotype, and $P < 0.0001$ for the interaction in (J). *$P < 0.05$, **$P < 0.01$, and ***$P < 0.001$ versus control *wfs1ab*^{WT}; ##$P < 0.01$ versus *wfs1ab*^{KO} larvae; Dunnett's or Newman-Keuls test in (A), (C), (E), (G), and (I).

the density of mitochondria was not different between $Wfs1^{\Delta exon8}$ and $Wfs1^{WT}$ mice (fig. S4, A and B). However, the number of mitochondria in contact with ER was greatly reduced in the mutant mice (fig. S4, A and C), confirming the phenotype seen previously in patient's fibroblasts. Then, we investigated the alterations of Ca^{2+} uptake and mitochondrial functionality using primary cultures of hippocampal and cortical neurons from $Wfs1^{\Delta exon8}$ mice (fig. S5). The cultures contained neurons as highlighted by the neuronal marker β3-tubulin (fig. S5, A and B). Neurons were stimulated with 10 μM glutamate, a physiological concentration innocuous to neurons (*48*), to evoke ER-Ca^{2+} release, and Ca^{2+} fluxes were analyzed in the mitochondria and cytosol using aequorin sensors. In response to glutamate, hippocampal and cortical neurons from $Wfs1^{\Delta exon8}$ mice released significantly less Ca^{2+} from the ER than $Wfs1^{WT}$ mice into the cytosol (P = 0.0040 in hippocampus and P = 0.0002 in cortex; fig. S5, D and H) and into the mitochondria (P = 0.0004 in hippocampus and P < 0.0001 in cortex; fig. S5, F and J). Ca^{2+} uptake by mitochondria drives several metabolic pathways and particularly Krebs cycle enzymes that provide cofactors to the mitochondrial respiratory chain and consequently control the energy production (*49*). Cells from patients with WS exhibited altered mitochondrial functionality with defects in complex I– and complex II–driven respiration, resulting in decreased oxygen consumption (*17*). Hence, we assessed the cellular bioenergetic response using a Seahorse analyzer, which permits the real-time monitoring of the oxygen consumption rate (OCR) under resting condition and after addition of manipulators of the mitochondrial respiratory chain: oligomycin [inhibitor of adenosine 5′-triphosphate (ATP) synthase], carbonyl cyanide-4 (trifluoromethoxy) phenylhydrazone (FCCP; uncoupler agent), and a mixture of rotenone (complex I inhibitor) and antimycin A (cytochrome c reductase inhibitor). As shown in fig. S5 (K to R), both hippocampal and cortical neurons from $Wfs1^{\Delta exon8}$ mice showed statistically significant decreases in basal OCR [P = 0.0071 (fig. S5, K and L) and P = 0.0003 (fig. S5, O and P)], in decoupled ATP-related rate [P = 0.0089 (fig. S5, K and M) and P < 0.0001 (fig. S5, O and Q)], and in maximal rate [P = 0.0341 (fig. S5, K and N) and P = 0.0327 (fig. S5, O and R)]. These data confirmed coherent alterations in neurons from $Wfs1^{\Delta exon8}$ mice and in patients' fibroblasts.

Therefore, in line with the clinical potentiality of S1R activation in WS, we assessed directly in human fibroblasts the impacts of PRE-084 on the deficits in Ca^{2+} uptake and mitochondrial functionality. We first performed the aequorin experiments in cells stimulated with Bradykinin, the inductor of Ca^{2+} release from the ER. In response to Bradykinin, fibroblasts from patients with WS released less Ca^{2+} from the ER than control fibroblasts. The amount of Ca^{2+} accumulated into the cytosol (−9%, P = 0.0466; Fig. 7, A, B, and D) and the Ca^{2+} taken up into the mitochondria (−20%, P = 0.0288; Fig. 7, E, F, and H) was reduced. These results are coherent with our previous observations (*17*) and assess that WFS1 loss impaired Ca^{2+} signaling directly at the IP_3R. PRE-084 was applied to cells in the 0.03 to 1 μM concentration range. The drug treatment increased, in a concentration-dependent manner, Ca^{2+} transfer into the cytosol not only in control cells but also in WS cells [P < 0.0001 with 1 μM PRE-084 as compared to V-treated Ct cells (Fig. 7C); P = 0.0004 with 1 μM PRE-084 as compared with WS cells (Fig. 7D)]. A similar effect was observed for Ca^{2+} transfer into the mitochondria [P = 0.0325 with 0.1 μM PRE-084 and P = 0.0054 with 1 μM as compared to V-treated Ct cells (Fig. 7G); P = 0.0365 with 0.1 μM PRE-084 and P = 0.0011 with 1 μM as compared with WS cells (Fig. 7H)]. At the highest dose tested, Ca^{2+} transfers were restored up to the values observed in control cells, suggesting a complete recovery of MAM functionality.

Mitochondrial function in cultured fibroblasts revealed a statistically significant decrease in basal OCR (−37%, P < 0.0001; Fig. 7, I and J), in decoupled ATP-related rate (−27%, P = 0.0029; Fig. 7, I and K), and in maximal rate (−42%, P = 0.0045; Fig. 7, I and L). PRE-084 treatment attenuated, in a concentration-dependent manner and significantly at 1 μM, the decreases in basal (P = 0.0127; Fig. 7J) and ATP-producing conditions (P = 0.0485; Fig. 7K). No effect was observed for the maximal rate (P = 0.1286; Fig. 7L). These observations demonstrated that increasing S1R activity restored Ca^{2+} transfer between ER and mitochondria and improved mitochondrial respiration in fibroblasts from patients with WS.

S1R agonist corrected the increased autophagy and mitophagy in WS human cells

Consequently, our efforts were dedicated to verify whether these improvements in Ca^{2+} exchanges could modulate a specific cellular pathway. WFS1 deficiency affects different cellular mechanisms, including cell proliferation, neuroinflammation, metabolic stress, and apoptosis, only to cite a few (*18*, *41*, *50*). Furthermore, a recent work demonstrated that the dysfunction in Ca^{2+} transmission associated with WFS1 down-regulation also determined dysregulation of mitochondrial dynamics and, in particular, altered the autophagic process (*51*).

To detect the autophagic events, we used the specific autophagic marker light chain 3 (MAP1LC3; hereafter referred to as LC3). When autophagy is induced, the cytoplasmic form of this protein (LC3-I) is cleaved and lipidated into the membrane-bound form (LC3-II), which anchors to the autophagic vesicle (*52*). This conversion may be detected with either live microscopy technique by transfecting cells with the green fluorescent protein (GFP)–LC3 construct or by Western immunoblot with specific antibodies against LC3 (*53*). Autophagosomes can thus be visualized as ring-shaped or punctate structures. Alternatively, the immunoblot analysis usually identifies two bands at 16 kDa (LC3-I) and 14 kDa (LC3-II). The LC3-II form correlates well with the autophagosome abundance and represents a reliable indicator of autophagy. We first analyzed whether $Wfs1^{\Delta exon8}$ mouse hippocampal and cortical neurons showed increased autophagy. Immunoblot analyses revealed an increased amount of LC3-II in $Wfs1^{\Delta exon8}$ neurons in the hippocampus (fig. S6, A and B) and in the cortex (fig. S6, C and D), confirming a coherent alteration as observed in a rat model (*51*). On the basis of these data, we further investigated whether fibroblasts from patients with WS bearing WFS1-null mutation could also present impairments in autophagy. Fluorescence microscopy analysis of autophagy with the GFP-LC3 reporter suggested that the WFS1 deficiency condition had significantly more abundant green punctate structures than WT samples (P < 0.0001; Fig. 8, A and B). This was confirmed by immunoblot analysis, where increased amounts of LC3-II were found in WFS1 KO fibroblasts (Fig. 8C). An increase in autophagic structures is not always representative of a condition where autophagy is sustained, but it can also be due to an alteration in the correct execution of the autophagic flux. In the present study, for example, the increases in LC3-II (found with the immunoblot approach) and in autophagosomal structured punctate (visualized by fluorescent microscopy) may, in theory, represent a failure of the autophagic

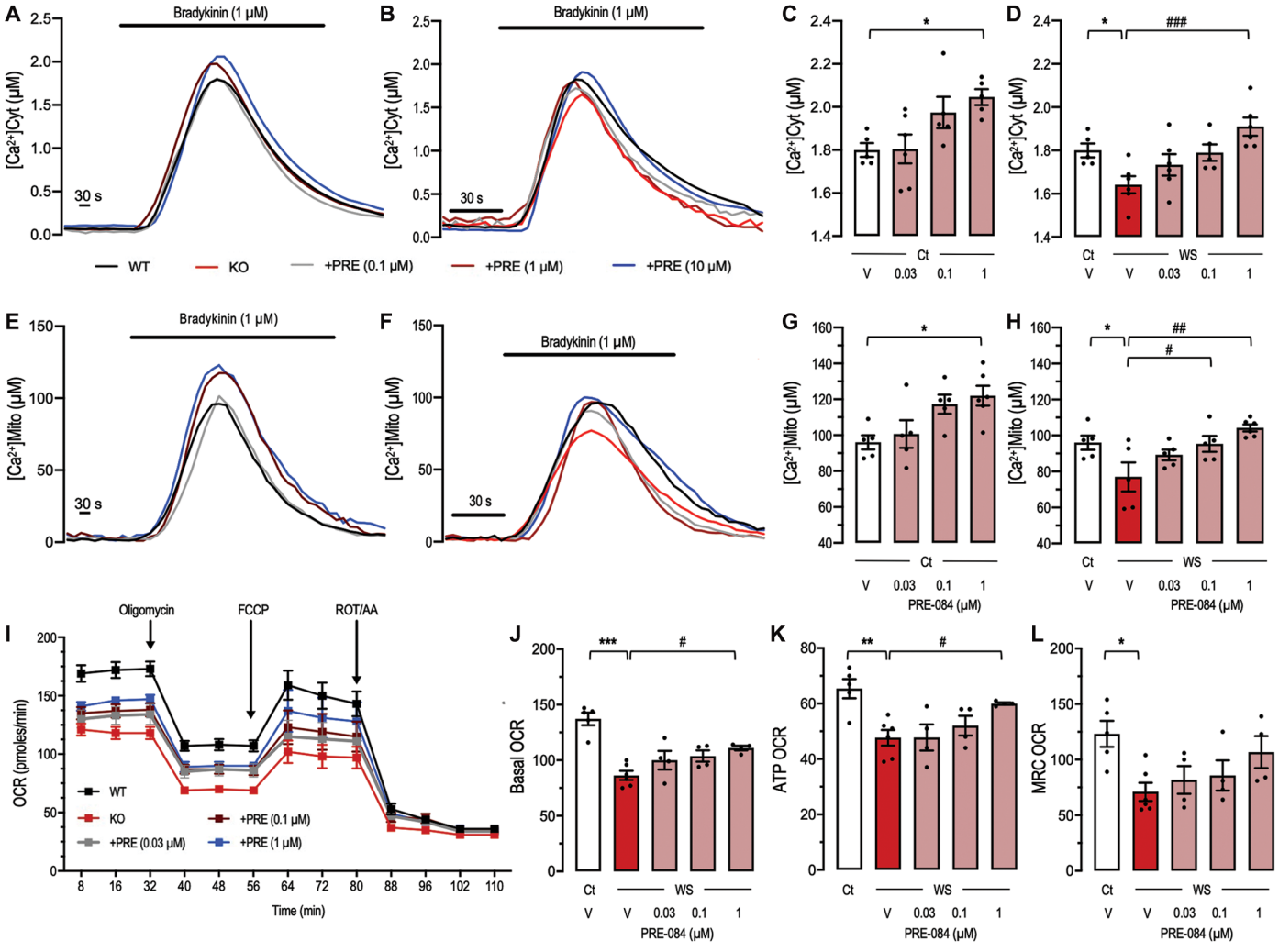

Fig. 7. PRE-084 restored the alterations of Ca^{2+} transfer from the ER and attenuated mitochondrial respiration deficits observed in fibroblasts derived from patients with WS. Representative traces of aequorin-based measurements of (**A** and **B**) cytosolic Ca^{2+} and (**C** and **D**) mitochondrial Ca^{2+} uptake, induced in fibroblasts from controls (Ct, black line) and patient with WS (red line). Ca^{2+} transfer was induced by stimulation with 1 μM Bradykinin and PRE-084 treatment: 0.1 μM (gray line), 1 μM (brown line), and 10 μM (blue line) on control (left) and patients with WS (right). Quantifications for (**E** and **F**) cytosolic Ca^{2+} and (**G** and **H**) mitochondrial Ca^{2+} uptake are expressed as means ± SEM of five independent experiments for each cell line. (**I**) Oxygen consumption rate (OCR) traces of control (Ct, black line) and patient fibroblasts (WS, red line), expressed as picomoles of O_2 per minute, under basal conditions and after the injection of oligomycin (1.5 μM), FCCP (1 μM), and ROT/AA (1 μM). PRE-084 was tested at 0.03 μM (gray line), 0.1 μM (purple line), and 1 μM (blue line). Quantifications of (**J**) basal, (**K**) ATP-related, and (**L**) maximal respiration rates were calculated from OCR traces and expressed as means ± SEM from five independent determinations. $n = 5$ to 6 per group in (A) to (H) and 4 to 6 in (I) to (L). One-way ANOVAs: $P < 0.05$ in (E); $P < 0.01$ in (F); $P < 0.05$ in (G); $P < 0.01$ in (H); $P < 0.0001$ in (J); $P < 0.01$ in (K); $P < 0.05$ in (L). $^{*}P < 0.05$, $^{**}P < 0.01$, and $^{***}P < 0.001$ versus V-treated Ct cells; #$P < 0.05$, ##$P < 0.01$, and ###$P < 0.001$ versus V-treated WS cells; Dunnett's test. FCCP, carbonyl cyanide-4 (trifluoromethoxy) phenylhydrazone; ROT/AA, rotenone/antimycin A.

machinery to fuse with lysosome or an impairment in lysosomal functions. To exclude this possibility, experiments were also performed with bafilomycin A1 (BafA1), which inhibits the late phase of autophagy. BafA1 inhibits autophagosome maturation by preventing the fusion of the autophagic vesicle with lysosomes. Results from fluorescence microscopy analysis and immunoblot demonstrated that BafA1 treatments in either WT or WFS1 KO sample were similarly characterized by abundant autophagosomal structures and lipidated LC3 form. Overall, these similarities in autophagosome accumulations indicated that WFS1 KO cells have the same sustained autophagosome formation process, which is not different from that seen in the WT. In other words, the normal autophagolysosomal processes are not compromised because of the pathological deletion of *WFS1* gene (Fig. 8, A to C). Thus, the increase in LC3-II and the autophagosome punctates seen in the WFS1 KO sample must be from other factors unrelated to the fusion of autophagosome and lysosome.

Thus, we reasoned that the reduced Ca^{2+} transfer from the ER into the mitochondria may represent a reasonable mechanism whereby the WFS1 KO sample may display an increase in autophagosome. Alteration of the normal Ca^{2+} transmission between the ER and the mitochondria represents a condition in which autophagy is activated (*54*). In this case, the reduced mitochondrial Ca^{2+} entry is not sufficient to activate the mitochondrial metabolism and to produce energy in ATP form. As a response, autophagy is activated to supply the cellular ATP demand. Because we denoted that

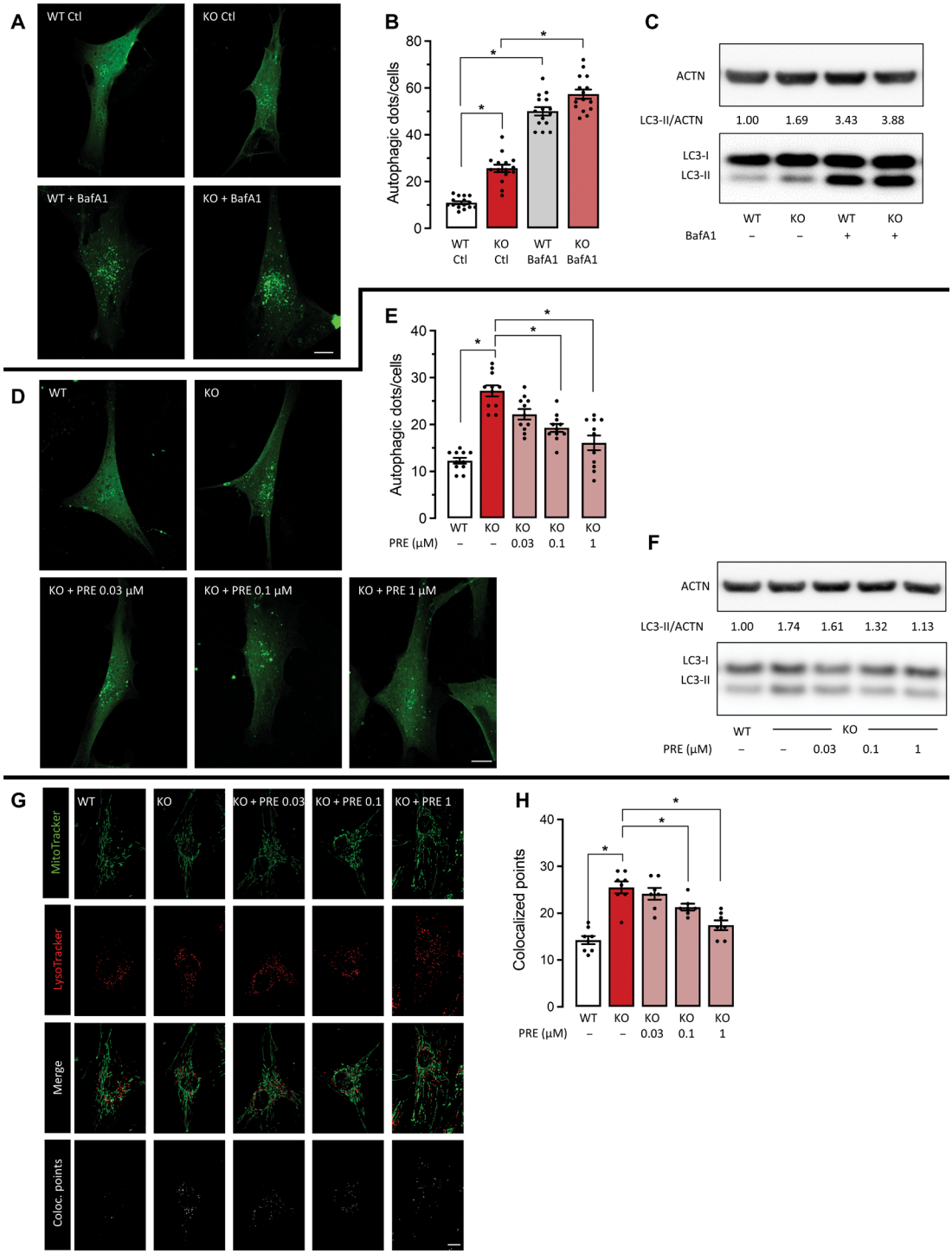

Fig. 8. PRE-084 restored the autophagy and mitophagy defects observed in fibroblasts derived from patients with WS. (**A** to **C**) Autophagy in fibroblasts of patients: (A) typical fluorescence microscopy images of fibroblasts from patients with WFS1-null mutation (KO), compared to WT cells, transfected with GFP-LC3 plasmid. (B) Quantification of LC3 vacuolated cells per field. (C) Representative immunoblot showing the increased LC3 lipidation (conversion of LC3-I to LC3-II) in fibroblasts from patients and control cells. Densitometry ratios of LC3-II over actin are shown and are relative to the control. In both experiments, the specific vacuolar H^+-dependent adenosine triphosphatase inhibitor bafilomycin A1 (BafA1) was added at a concentration of 100 nM for 2 hours to mimic a blockage of the autophagic flux. (**D** and **F**) PRE-084 reestablished the normal autophagic rates in fibroblasts from patients with WFS1-null mutation (KO) to a value similar to those observed in WT samples, as demonstrated by fluorescence microscopy analysis: (D) typical images and (**E**) quantification and by immunoblot (F). In both experiments, PRE-084 was used at the concentrations of 0.03, 0.1, and 1 µM. Densitometry ratios of LC3-II over actin are shown and are relative to the control. (**G** and **H**) Mitophagy activation was analyzed by confocal microscopy with the specific mitochondrial and lysosomal markers, MitoTracker Green and LysoTracker Red, in fibroblasts from patients, with WFS1-null mutation (KO) and WT fibroblasts. (G) Representative images of the colocalization points and (H) quantification. Scale bars, 10 µm in (A), (D), and (G). $n = 15$ per group in (B), 11 in (E), and 7 to 8 in (H). (B) Two-way ANOVA: $P < 0.0001$ for the genotype, $P < 0.0001$ for the BafA1 treatment, and $P < 0.05$ for the interaction in (B). One-way ANOVAs: $P < 0.0001$ in (E); $F_{(4,32)} = 20.21$ and $P < 0.0001$ in (H). *$P < 0.05$ versus WT cells; Dunnett's test.

WSF1-deficient samples had a reduced ER-mitochondrial Ca^{2+} transmission and a decreased mitochondrial functioning and energetic production and that the S1R agonist induced a functional recovery, we investigated the possible impact of PRE-084 treatment on autophagy. We observed that the PRE-084 reduced, in a concentration-dependent manner, the excessive autophagia seen in WSF1 KO cells using fluorescence microscopy (−74%, $P < 0.0001$ with 1 µM PRE-084 as compared with V-treated WS cells; Fig. 8, D and E) and immunoblotting (−82%; Fig. 8F). At the highest dose tested, autophagy was closer to the one observed in control cells. Next, we

monitored the mitophagy, the specialized form of autophagy responsible for the mitochondrial removal (*55*). We assessed mitophagy with confocal fluorescence microscopy by the simultaneous labeling of autophagolysosomes and mitochondria with fluorescent probes. KO samples presented an increased mitophagic activation (Fig. 8, G and H). PRE-084 attenuated the excessive mitochondrial removal, and posttreatment mitochondrial removal rates were comparable to those observed in WT fibroblasts (Fig. 8, G and H).

DISCUSSION

WS is a multisystem pathology in which metabolic, auricular, ocular, cognitive, and mood manifestations contribute to the severity of the disease. Therapeutic interventions for the treatment of WS are currently only palliative. Proposed strategies focus mainly on drug repurposing, which could alleviate one or several symptoms but with a very limited landscape of possible hits, or on gene therapy using genome editing (*56*). The latter strategy aims at defining an effective regenerating therapy, but it may imply high development costs for such a rare disease. The most straightforward strategy to correct the cellular deficit would be to restore WFS1 expression using human gene transfer. Because WS is due to a loss of function, classical gene therapy approach that would express the defective protein should correct the alterations. However, a limitation of this strategy is the expression of WFS1 in the affected organs (retina, cochlea, pons, hippocampus, and pancreas) and into the right cells. The selection of a pertinent vector with the appropriate promoter brings difficulties to this seducing approach. Another strategy could be to target NCS1. In WS, NCS1 protein amount is decreased. This diminution alters the proper functioning of IP_3R, thus provoking a reduction of the Ca^{2+} concentration in the mitochondrial matrix and alterations of complex I and II activities in the respiratory chain. These dysfunctions are associated with an alteration of the MAM structure (*17*, *18*, *20*). In vitro, overexpression of NCS1 in WS fibroblasts corrected the cellular deficits (*17*). Therefore, a gene therapy approach targeting NCS1 may give promising results. The issues, however, would be similar to those expected for *WFS1*-targeting gene therapy.

A better alternative would be to identify target proteins in MAMs that could be addressed with small, clinically developable molecules that could permit a cellular functional recovery. We here identified S1R as such a pertinent target and reported that S1R overexpression or treatment with a reference agonist, PRE-084 (*37*, *39*), increased Ca^{2+} transfer from the ER to the mitochondria or cytosol and improved mitochondrial function in WS fibroblasts in vitro. The drug also decreased locomotor alterations, cognitive deficits, and anxiety in mouse and zebrafish models of WS in vivo. S1R is an effective modulator of IP_3R (*31*, *57*) and interacts with several proteins involved in ER-mitochondria Ca^{2+} transfer and/or activation of the ER stress (*29*). By stabilizing the conformation of IP_3R at the MAMs, it increases Ca^{2+} efflux into the mitochondria (*31*, *58*). S1R activation directly controls mitochondrial respiration and generation of mitochondrial reactive oxygen species. The facts that S1R is expressed rather ubiquitously in numerous cell types and that it can be activated/inactivated by small druggable molecules explain the increasing number of preclinical and clinical developments currently in progress (*43*).

We used the S1R agonist PRE-084, known to potentiate Ca^{2+} transfer from the ER to the cytosol in NG-108 cells (*31*). We confirmed its effect in control fibroblasts and showed that it was still observable in fibroblasts derived from patients with WS, thus presenting a therapeutic interest. PRE-084 increased not only the intracellular Ca^{2+} accumulation but also the ability of mitochondria to take up Ca^{2+}, in accordance with previous observations (*31*, *59*). An increase in the mitochondrial Ca^{2+} quantity positively regulates the activities of the Krebs cycle enzymes and of components of the mitochondrial electron transport chain (*60*, *61*). As a result, mitochondrial metabolism and ATP production were boosted, with a consequent increase in cellular energetics. Different investigations highlighted how deregulations in Ca^{2+} transfer into the mitochondrial compartment also contributed to different human diseases (*62*), including neurodegeneration (*63*, *64*). Restoration of the mitochondrial Ca^{2+} homeostasis was found to be sufficient to promote beneficial effect (*65*). We measured OCR before and after PRE-084. The S1R agonist allowed a functional recovery of mitochondrial respiration linked to ATP production and a reactivation of Ca^{2+} dynamics, suggesting that this effect was related to the alleviation of pathological symptoms in vivo. Our work focused on S1R's role on MAM physiology. However, several other functions for S1R have been described in the literature. S1R increased brain-derived neurotrophic factor (BDNF) release (*47*, *66*), regulated cellular excitability through plasma membrane channel (*67*, *68*), and modulated the cholesterol lipid scaffolding at MAMs (*69*). In addition, S1R has been shown to regulate dopamine receptor and transporters (*70*), and dopaminergic alterations have been described in *Wfs1*$^{\Delta exon8}$ mice (*71*, *72*). However, such an effect could be ruled out, because PRE-084 or S1R overexpression would have increased the dopamine concentration and led to increased locomotion in zebrafish (*73*). Furthermore, in mice, PRE-084 at 0.3 mg/kg (the dose used in our experiments) was shown not to affect dopamine concentration even after 90 min (*44*).

Restoration of Ca^{2+} transmission by increasing concentrations of PRE-084 also controlled the autophagic and mitophagic mechanisms critical for mitochondrial functioning. Reduced mitochondrial Ca^{2+} entry triggers autophagic processes to increase the energy production under different cellular conditions and diseases (*74*). A WSF1 down-regulation and consequent alteration of the Ca^{2+} dynamics and mitochondrial homeostasis also activated the autophagic processes (*51*). Our data confirmed that loss of WSF1 increased autophagy and mitophagy. In neurodegeneration, mitophagy represents a double-edge sword (*74*). Mitophagy controls the mitochondrial turnover and warrants the presence of a healthy mitochondrial population, but excessive mitophagy is detrimental for proper cellular functioning and survival. Our data support the notion that proper Ca^{2+} signaling from the ER to the mitochondria, mediated by S1R at the MAM, plays a functional recovery role against the increased autophagy and mitophagy.

These findings open potential therapeutic opportunities in which specific autophagic modulators may be combined with S1R agonists to combat WS. Modulators of autophagy are already clinically approved for different human diseases. However, further studies are needed. First, it will be necessary to check that the effects of S1R agonists on autophagy observed in fibroblasts are maintained in more specialized cell types that are primary targets of WFS1 mutations, such as neurons and myocytes. Then, because autophagy and mitophagy inhibition may be complementally beneficial to the function of S1R agonist in the treatment of WS, it would be desirable to clarify the fundamental relationship between S1R and autophagy or mitophagy, which, at present, is not well understood (*75*–*78*).

Wfs1$^{\Delta Exon8}$ mice have a complex behavioral pattern in cognitive and mood responses, with some gender-related differences in impairment intensity. Analyses of learning and memory abilities of *Wfs1*$^{\Delta Exon8}$ mice showed deficits in spontaneous alternation, passive avoidance, and object recognition. This suggested that alterations of spatial and nonspatial, short-term, and long-term memories were not complete, because spatial information of the platform location measured during the water maze probe test was, for instance, not affected.

Anxiety responses of *Wfs1*$^{\Delta Exon8}$ mice also revealed mild gender-related differences because only female *Wfs1*$^{\Delta Exon8}$ mice showed decreases in locomotion in the center of the open field and in the time spent or time per visit in the aversive compartment of the elevated plus maze and of the light-dark exploration box. Mood disorders were suggested in male exon 2–targeted *Wfs1* KO mice by Kato *et al.* (*79*), due to alterations in passive avoidance conditioning, immobility duration during forced swimming, and social interaction. Luuk *et al.* (*15*) reported alteration of anxiety response, more particularly when animals were isolated, in the light-dark exploration box and elevated plus maze. We confirmed these observations and observed that these alterations are enhanced in females compared to males.

WFS1 deficiency leads to DM. This hyperglycemia is suspected to be associated with the progression of the disease in human (*1*). In a rat *Wfs1* KO model, Plaas *et al.* (*80*) observed a reduction of the β cell mass associated with hyperglycemia, but a direct link with the occurrence and/or progression of the neurodegenerative processes was not demonstrated. A specific experiment using a tissue-specific invalidation of Wfs1 restricted to the pancreas and subsequent analysis of the resulting anomalies would be an important step to address this important question.

These hallmarks are consistent with the symptomatology of WS, although no gender-related differences have been reported in patients. Cognitive performance deficits were identified in cohort studies and in individual clinical case reports. *WFS1* gene has been suggested to have a role in the susceptibility for mood disorders (*81*).

The treatment with PRE-084 was able to attenuate, if not completely restore, learning deficits in male *Wfs1*$^{\Delta Exon8}$ mice and anxiety responses in female *Wfs1*$^{\Delta Exon8}$ mice. This was observed after an acute treatment at a dose previously shown to be antiamnesic (*37*, *82*) and neuroprotective in preclinical models of Alzheimer's disease (*45*), Huntington's disease (*83*), Parkinson's disease (*47*), and amyotrophic lateral sclerosis (*84*). The drug also blocked the hyperactivity observed in *wfs1ab*^{KO} zebrafish larvae. Loss of Wfs1 function led to hypomobility in mouse and hypermobility in zebrafish larvae. Animal mobility is a typical ethological response and relies on different physiological substrata between fish and rodents. The anxiety in mouse is associated with hypolocomotion (*85*). In contrast, in zebrafish larvae, anxiety behavior after abrupt changes in light intensity is associated with a hyperlocomotor response (*86*–*88*). It is therefore expected that the invalidation of a target could lead to a different behavioral phenotypic response in different animals. Moreover, the drug effect was not only prevented by the selective S1R antagonist NE-100 but also mimicked by direct overexpression of S1R. These observations confirmed the pharmacological importance of S1R activity in the restoration of WS symptoms. The drug effect must be, however, confirmed in other major WS symptoms (diabetes, OA, and deafness) that will have to be characterized in complementary animal models.

A few limitations could be identified in the present study, and some aspects will deserve more investigations in the future. First is the efficacy in correcting all symptoms associated with WS, namely diabetes, hearing loss, and OA. We were limited to the symptomatology shown by the available preclinical animal models, and none of them fully described the human symptomatology. It was the reason why we combine different analyses in both zebrafish and mouse models. None of these in vivo models were tested for visual impairments, auditory defects, or glucose regulation. It will be important to address these issues in future studies, because the primary outcomes in clinical trials must address pathologically pertinent symptoms. For instance, the active trials NCT02841553 and NCT03717909 address changes in C-peptide levels or visual acuity, respectively.

Moreover, we used PRE-084 to provide a proof of concept that S1R activation is a relevant therapeutic strategy to treat WS. The drug is a prototypic S1R agonist, shown to be effective in numerous neurodegenerative disorders (*38*, *45*, *47*, *84*), but it is only a pharmacological tool used in investigational research that will not be developed at the clinical stage. A selective, effective, bioavailable, and innocuous S1R agonist has yet to be proposed and developed at the clinical stage. Moreover, we used an acute injection protocol with PRE-084 in mice experiments. Translation in humans will require further preclinical and clinical analyses of the efficacy and consequences of long-term S1R activation in WS, because it would be chronically administered in humans to ameliorate the symptoms.

Last, S1R activation is known to result in pleiotropic cellular effects (*30*, *43*). The consequence of S1R activation in correcting most of the cellular and behavioral deficits was coherently related to MAM function that is primarily altered in WS. However, S1R is also supposed to play numerous other cellular functions, including release of BDNF and modulation of membrane channels and transporters, and that would require further evaluation to comprehensively understand whether S1R acts on other signaling pathways. For instance, the role of S1R on dopamine receptors and transporter activity, although it was unlikely to be involved in the observed effects, deserves further study. In addition, the impact of the hyperglycemia on the observed phenotype in WS models would merit the analysis of the behavior in a pancreas-specific Wfs1-deficient mice. Together, these limitations could be easily addressed in a future translational program aiming at clinically developing a selective S1R agonist in WS and related pathologies.

From the present observations, we anticipate that the ER-mitochondria communication deficit in tissues and organs, the hallmark of WS, is likely to be improved upon treatment with S1R agonists in patients with WS. We demonstrated that MAM deficit in a prototypic monogenic MAM disorder could be functionally attenuated by a pharmacological strategy targeting another MAM-resident protein with a similar function.

MATERIALS AND METHODS

Study design

We first conducted a behavioral phenotyping of male and female *Wfs1*$^{\Delta Exon8}$ mice at 3 months of age using behavioral tests measuring mobility, memory, and anxiety. It revealed that, although animals are known not to present diabetes, OA, or deafness at this age, they showed neurological and psychiatric deficits resulting in hypolocomotion, learning deficits, and anxiety. We analyzed WFS1, NCS1, and S1R expression in the hippocampus and cortex of the mice, using reverse transcription polymerase chain reaction (RT-PCR) and Western blotting, and compared with NCS1 and WFS1 expression

in S1R KO mice to determine whether targeting S1R activity could be relevant. We tested the pharmacological effect of the reference S1R agonist against the learning deficits in males and anxiety responses in females. To confirm the in vivo data in mice, we used the *Wfs1ab*^{KO} zebrafish model that presents an altered locomotor response to visual stimulation. We confirmed the PRE-084 effect and compared with overexpression of S1R in the zebrafish line. Last, to show that the beneficial S1R activity was related to a functional effect on MAMs, we used fibroblast from patients with WS to analyze PRE-084's effect on Ca^{2+} transfer from the ER to the cytosol or mitochondria and the consequences on mitochondrial respiratory capacities and its related increased autophagy and mitophagy.

The sample size used in each experiment was predefined by power calculations using G*Power software (setting the effect size at 1.3, α at 0.05, and power at 0.8) and was routinely 10 to 15 for in vivo analyses and 4 to 6 for in vitro analyses. All animal procedures were conducted in strict adherence to the European Union Directive 2010/63 and authorized by the National Ethic Committee (Paris) (APAFIS no. 2018051411079082 #15035) or in accordance with the guidelines of the National Institutes of Health and the National Institute on Drug Abuse Intramural Research Program Animal Care and Use Program, which is fully accredited by the Association for Assessment and Accreditation of Laboratory Animal Care International. A priori exclusion criteria were followed in almost all of the procedures and are detailed for each test in Supplementary Materials and Methods. No outlier was discarded during statistical analysis. Data from successive experiments were pooled, not replicated, as routinely done for in vivo experiments. Mice were randomly assigned to the treatment groups. Experiments were not blinded, but data analysis was performed by a different experimenter.

Statistical analyses

The sample size was empirically determined and confirmed using the G-power v3.1.9.2 software (Faul, Erdfelder, Lang, and Buchner) taking into account the strength of the tests applied to the behavioral or biochemical responses (effect size = 1.3, α = 0.05, and power = 0.8). Data were analyzed using the Prism v9.1.1 software (GraphPad). Two-way analysis of variance (ANOVA) was used with gender and genotype as independent factors, followed by Newman-Keuls post hoc test. When a cutoff time was set, for passive avoidance latencies or water maze swimming durations, data do not follow a Gaussian distribution, and violin graphs showing median and interquartile range and nonparametric tests were used. Data were analyzed using Kruskal-Wallis ANOVA (*H* value) or a repeated-measures Friedman ANOVA (*Q* values), followed by Dunn's post hoc test. All ANOVA analyses are detailed in the Supplementary Materials. One-column comparisons versus chance or zero values (corresponding to 50% preference for object recognition or 15 s for the time spent in the pool quadrant) were performed using a one-column *t* test. The statistical significance was $P < 0.05$. For reading clarity, all statistical data are detailed in the figure legends and the Supplementary Materials.

SUPPLEMENTARY MATERIALS

www.science.org/doi/10.1126/scitranslmed.abh3763
Materials and Methods
Figs. S1 to S10
Data file S1
References (*89*–*96*)

View/request a protocol for this paper from *Bio-protocol*.

REFERENCES AND NOTES

1. J. Rohayem, C. Ehlers, B. Wiedemann, R. Holl, K. Oexle, O. Kordonouri, G. Salzano, T. Meissner, W. Burger, E. Schober, A. Huebner, M. A. Lee-Kirsch, G. Wolfram, Diabetes and neurodegeneration in Wolfram syndrome: A multicenter study of phenotype and genotype. *Diabetes Care* **34**, 1503–1510 (2011).
2. D. J. Wolfram, H. P. Wagener, Diabetes mellitus and simple optic atrophy among siblings: Report of four cases. *Mayo Clin. Proc.* **13**, 715–718 (1938).
3. T. G. Barrett, S. E. Bundey, A. F. Macleod, Neurodegeneration and diabetes: UK nationwide study of Wolfram (DIDMOAD) syndrome. *Lancet* **346**, 1458–1463 (1995).
4. A. Chaussenot, S. Bannwarth, C. Rouzier, B. Vialettes, S. A. Mkadem, B. Chabrol, A. Cano, P. Labauge, V. Paquis-Flucklinger, Neurologic features and genotype-phenotype correlation in Wolfram syndrome. *Ann. Neurol.* **69**, 501–508 (2011).
5. K. O. Rove, G. J. Vricella, T. Hershey, M. H. Thu, H. M. Lugar, J. Vetter, B. A. Marshall, P. F. Austin, Lower urinary tract dysfunction and associated pons volume in patients with wolfram syndrome. *J. Urol.* **200**, 1107–1113 (2018).
6. J. Xavier, N. Bourvis, A. Tanet, T. Ramos, D. Perisse, I. Marey, D. Cohen, A. Consoli, Bipolar disorder type 1 in a 17-year-old girl with Wolfram syndrome. *J. Child Adolesc. Psychopharmacol.* **26**, 750–755 (2016).
7. G. S. Gowda, D. Rai, R. K. Nadella, S. Tiwari, R. Yadav, S. B. Math, Schizophrenia in Wolfram syndrome (DIDMOAD syndrome): A case report in support of the mitochondrial dysfunction hypothesis. *Schizophr. Res.* **195**, 574–575 (2018).
8. A. Sequeira, C. Kim, M. Seguin, A. Lesage, N. Chawky, A. Desautels, M. Tousignant, C. Vanier, O. Lipp, C. Benkelfat, G. Rouleau, G. Turecki, Wolfram syndrome and suicide: Evidence for a role of WFS1 in suicidal and impulsive behavior. *Am. J. Med. Genet. B Neuropsychiatr. Genet.* **119B**, 108–113 (2003).
9. S. S. Chatterjee, S. Mitra, S. K. Pal, Mania in Wolfram's disease: From bedside to bench. *Clin Psychopharmacol Neurosci* **15**, 70–72 (2017).
10. H. Inoue, Y. Tanizawa, J. Wasson, P. Behn, K. Kalidas, E. Bernal-Mizrachi, M. Mueckler, H. Marshall, H. Donis-Keller, P. Crock, D. Rogers, M. Mikuni, H. Kumashiro, K. Higashi, G. Sobue, Y. Oka, M. A. Permutt, A gene encoding a transmembrane protein is mutated in patients with diabetes mellitus and optic atrophy (Wolfram syndrome). *Nat. Genet.* **20**, 143–148 (1998).
11. T. M. Strom, K. Hortnagel, S. Hofmann, F. Gekeler, C. Scharfe, W. Rabl, K. D. Gerbitz, T. Meitinger, Diabetes insipidus, diabetes mellitus, optic atrophy and deafness (DIDMOAD) caused by mutations in a novel gene (wolframin) coding for a predicted transmembrane protein. *Hum. Mol. Genet.* **7**, 2021–2028 (1998).
12. K. Cryns, S. Thys, L. Van Laer, Y. Oka, M. Pfister, L. Van Nassauw, R. J. Smith, J. P. Timmermans, G. Van Camp, The WFS1 gene, responsible for low frequency sensorineural hearing loss and Wolfram syndrome, is expressed in a variety of inner ear cells. *Histochem. Cell Biol.* **119**, 247–256 (2003).
13. J. Kawano, Y. Tanizawa, K. Shinoda, Wolfram syndrome 1 (Wfs1) gene expression in the normal mouse visual system. *J. Comp. Neurol.* **510**, 1–23 (2008).
14. S. G. Fonseca, M. Fukuma, K. L. Lipson, L. X. Nguyen, J. R. Allen, Y. Oka, F. Urano, WFS1 is a novel component of the unfolded protein response and maintains homeostasis of the endoplasmic reticulum in pancreatic beta-cells. *J. Biol. Chem.* **280**, 39609–39615 (2005).
15. H. Luuk, S. Koks, M. Plaas, J. Hannibal, J. F. Rehfeld, E. Vasar, Distribution of Wfs1 protein in the central nervous system of the mouse and its relation to clinical symptoms of the Wolfram syndrome. *J. Comp. Neurol.* **509**, 642–660 (2008).
16. D. Takei, H. Ishihara, S. Yamaguchi, T. Yamada, A. Tamura, H. Katagiri, Y. Maruyama, Y. Oka, WFS1 protein modulates the free Ca^{2+} concentration in the endoplasmic reticulum. *FEBS Lett.* **580**, 5635–5640 (2006).
17. C. Angebault, J. Fauconnier, S. Patergnani, J. Rieusset, A. Danese, C. A. Affortit, J. Jagodzinska, C. Megy, M. Quiles, C. Cazevieille, J. Korchagina, D. Bonnet-Wersinger, D. Milea, C. Hamel, P. Pinton, M. Thiry, A. Lacampagne, B. Delprat, C. Delettre, ER-mitochondria cross-talk is regulated by the Ca^{2+} sensor NCS1 and is impaired in Wolfram syndrome. *Sci. Signal.* **11**, eaaq1380 (2018).
18. B. Delprat, T. Maurice, C. Delettre, Wolfram syndrome: MAMs' connection? *Cell Death Dis.* **9**, 364 (2018).
19. C. Lopez-Crisosto, R. Bravo-Sagua, M. Rodriguez-Pena, C. Mera, P. F. Castro, A. F. Quest, B. A. Rothermel, M. Cifuentes, S. Lavandero, ER-to-mitochondria miscommunication and metabolic diseases. *Biochim. Biophys. Acta* **1852**, 2096–2105 (2015).
20. B. Delprat, J. Rieusset, C. Delettre, Defective endoplasmic reticulum–mitochondria connection is a hallmark of Wolfram syndrome. *Contact* **2**, 1–5 (2019).
21. S. Paillusson, R. Stoica, P. Gomez-Suaga, D. H. W. Lau, S. Mueller, T. Miller, C. C. J. Miller, There's something wrong with my MAM; the ER-mitochondria axis and neurodegenerative diseases. *Trends Neurosci.* **39**, 146–157 (2016).
22. H. Cheng, X. Gang, G. He, Y. Liu, Y. Wang, X. Zhao, G. Wang, The molecular mechanisms underlying mitochondria-associated endoplasmic reticulum membrane-induced insulin resistance. *Front Endocrinol (Lausanne)* **11**, 592129 (2020).
23. E. Tubbs, S. Chanon, M. Robert, N. Bendridi, G. Bidaux, M. A. Chauvin, J. Ji-Cao, C. Durand, D. Gauvrit-Ramette, H. Vidal, E. Lefai, J. Rieusset, Disruption of mitochondria-associated

endoplasmic reticulum membrane (MAM) integrity contributes to muscle insulin resistance in mice and humans. *Diabetes* **67**, 636–650 (2018).
24. P. Gao, Z. Yan, Z. Zhu, Mitochondria-associated endoplasmic reticulum membranes in cardiovascular diseases. *Front. Cell Dev. Biol.* **8**, 604240 (2020).
25. R. Medlej, J. Wasson, P. Baz, S. Azar, I. Salti, J. Loiselet, A. Permutt, G. Halaby, Diabetes mellitus and optic atrophy: A study of Wolfram syndrome in the Lebanese population. *J. Clin. Endocrinol. Metab.* **89**, 1656–1661 (2004).
26. T. Nickl-Jockschat, H. J. Kunert, B. Herpertz-Dahlmann, M. Grozinger, Psychiatric symptoms in a patient with Wolfram syndrome caused by a combination of thalamic deficit and endocrinological pathologies. *Neurocase* **15**, 47–52 (2008).
27. A. Waschbisch, B. Volbers, T. Struffert, J. Hoyer, S. Schwab, J. Bardutzky, Primary diagnosis of Wolfram syndrome in an adult patient--case report and description of a novel pathogenic mutation. *J. Neurol. Sci.* **300**, 191–193 (2011).
28. A. N. Bischoff, A. M. Reiersen, A. Buttlaire, A. Al-Lozi, T. Doty, B. A. Marshall, T. Hershey, G. Washington, Selective cognitive and psychiatric manifestations in Wolfram syndrome. *Orphanet J. Rare Dis.* **10**, 66 (2015).
29. T. Hayashi, T. P. Su, Sigma-1 receptor chaperones at the ER-mitochondrion interface regulate Ca^{2+} signaling and cell survival. *Cell* **131**, 596–610 (2007).
30. T. P. Su, T. Hayashi, T. Maurice, S. Buch, A. E. Ruoho, The sigma-1 receptor chaperone as an inter-organelle signaling modulator. *Trends Pharmacol. Sci.* **31**, 557–566 (2010).
31. T. Hayashi, T. Maurice, T. P. Su, Ca^{2+} signaling via ς_1-receptors: Novel regulatory mechanism affecting intracellular Ca^{2+} concentration. *J. Pharmacol. Exp. Ther.* **293**, 788–798 (2000).
32. T. Maurice, N. Goguadze, Sigma-1 (σ_1) receptor in memory and neurodegenerative diseases. *Handb. Exp. Pharmacol.* **244**, 81–108 (2017).
33. V. Lahmy, R. Long, D. Morin, V. Villard, T. Maurice, Mitochondrial protection by the mixed muscarinic/σ_1 ligand ANAVEX2-73, a tetrahydrofuran derivative, in $A\beta_{25-35}$ peptide-injected mice, a nontransgenic Alzheimer's disease model. *Front. Cell. Neurosci.* **8**, 463 (2015).
34. V. Lahmy, J. Meunier, S. Malmstrom, G. Naert, L. Givalois, S. H. Kim, V. Villard, A. Vamvakides, T. Maurice, Blockade of tau hyperphosphorylation and $A\beta_{1-42}$ generation by the aminotetrahydrofuran derivative ANAVEX2-73, a mixed muscarinic and σ_1 receptor agonist, in a nontransgenic mouse model of Alzheimer's disease. *Neuropsychopharmacology* **38**, 1706–1723 (2013).
35. V. Villard, J. Espallergues, E. Keller, T. Alkam, A. Nitta, K. Yamada, T. Nabeshima, A. Vamvakides, T. Maurice, Antiamnesic and neuroprotective effects of the aminotetrahydrofuran derivative ANAVEX1-41 against amyloid β_{25-35}-induced toxicity in mice. *Neuropsychopharmacology* **34**, 1552–1566 (2009).
36. V. Villard, J. Espallergues, E. Keller, A. Vamvakides, T. Maurice, Anti-amnesic and neuroprotective potentials of the mixed muscarinic receptor/sigma$_1$(σ_1) ligand ANAVEX2-73, a novel aminotetrahydrofuran derivative. *J. Psychopharmacol.* **25**, 1101–1117 (2011).
37. T. Maurice, T. P. Su, D. W. Parish, T. Nabeshima, A. Privat, PRE-084, a sigma selective PCP derivative, attenuates MK-801-induced impairment of learning in mice. *Pharmacol. Biochem. Behav.* **49**, 859–869 (1994).
38. Z. Y. Motawe, S. S. Abdelmaboud, J. Cuevas, J. W. Breslin, PRE-084 as a tool to uncover potential therapeutic applications for selective sigma-1 receptor activation. *Int. J. Biochem. Cell Biol.* **126**, 105803 (2020).
39. T. P. Su, X. Z. Wu, E. J. Cone, K. Shukla, T. M. Gund, A. L. Dodge, D. W. Parish, Sigma compounds derived from phencyclidine: Identification of PRE-084, a new, selective sigma ligand. *J. Pharmacol. Exp. Ther.* **259**, 543–550 (1991).
40. S. Koks, U. Soomets, J. L. Paya-Cano, C. Fernandes, H. Luuk, M. Plaas, A. Terasmaa, V. Tillmann, K. Noormets, E. Vasar, L. C. Schalkwyk, Wfs1 gene deletion causes growth retardation in mice and interferes with the growth hormone pathway. *Physiol. Genomics* **37**, 249–259 (2009).
41. L. Rigoli, P. Bramanti, C. Di Bella, F. De Luca, Genetic and clinical aspects of Wolfram syndrome 1, a severe neurodegenerative disease. *Pediatr. Res.* **83**, 921–929 (2018).
42. E. De Franco, S. E. Flanagan, T. Yagi, D. Abreu, J. Mahadevan, M. B. Johnson, G. Jones, F. Acosta, M. Mulaudzi, N. Lek, V. Oh, O. Petz, R. Caswell, S. Ellard, F. Urano, A. T. Hattersley, Dominant ER stress-inducing WFS1 mutations underlie a genetic syndrome of neonatal/infancy-onset diabetes, congenital sensorineural deafness, and congenital cataracts. *Diabetes* **66**, 2044–2053 (2017).
43. T. Maurice, Bi-phasic dose response in the preclinical and clinical developments of sigma-1 receptor ligands for the treatment of neurodegenerative disorders. *Expert Opin Drug Discov* **16**, 373–389 (2021).
44. L. Garces-Ramirez, J. L. Green, T. Hiranita, T. A. Kopajtic, M. Mereu, A. M. Thomas, C. Mesangeau, S. Narayanan, C. R. McCurdy, J. L. Katz, G. Tanda, Sigma receptor agonists: Receptor binding and effects on mesolimbic dopamine neurotransmission assessed by microdialysis. *Biol. Psychiatry* **69**, 208–217 (2011).
45. J. Meunier, J. Ieni, T. Maurice, The anti-amnesic and neuroprotective effects of donepezil against amyloid β_{25-35} peptide-induced toxicity in mice involve an interaction with the σ_1 receptor. *Br. J. Pharmacol.* **149**, 998–1012 (2006).
46. T. Maurice, V. L. Phan, A. Privat, The anti-amnesic effects of sigma$_1$ (σ_1) receptor agonists confirmed by in vivo antisense strategy in the mouse. *Brain Res.* **898**, 113–121 (2001).
47. V. Francardo, F. Bez, T. Wieloch, H. Nissbrandt, K. Ruscher, M. A. Cenci, Pharmacological stimulation of sigma-1 receptors has neurorestorative effects in experimental parkinsonism. *Brain* **137**, 1998–2014 (2014).
48. N. Plotegher, D. Perocheau, R. Ferrazza, G. Massaro, G. Bhosale, F. Zambon, A. A. Rahim, G. Guella, S. N. Waddington, G. Szabadkai, M. R. Duchen, Impaired cellular bioenergetics caused by GBA1 depletion sensitizes neurons to calcium overload. *Cell Death Differ.* **27**, 1588–1603 (2020).
49. S. Marchi, M. Bittremieux, S. Missiroli, C. Morganti, S. Patergnani, L. Sbano, A. Rimessi, M. Kerkhofs, J. B. Parys, G. Bultynck, C. Giorgi, P. Pinton, Endoplasmic reticulum-mitochondria communication through Ca^{2+} signaling: The importance of mitochondria-associated membranes (MAMs). *Adv. Exp. Med. Biol.* **997**, 49–67 (2017).
50. F. Urano, Wolfram syndrome: Diagnosis, management, and treatment. *Curr. Diab. Rep.* **16**, 6 (2016).
51. M. Cagalinec, M. Liiv, Z. Hodurova, M. A. Hickey, A. Vaarmann, M. Mandel, A. Zeb, V. Choubey, M. Kuum, D. Safiulina, E. Vasar, V. Veksler, A. Kaasik, Role of mitochondrial dynamics in neuronal development: Mechanism for Wolfram syndrome. *PLoS Biol.* **14**, e1002511 (2016).
52. S. Patergnani, S. Marchi, A. Rimessi, M. Bonora, C. Giorgi, K. D. Mehta, P. Pinton, PRKCB/protein kinase C, beta and the mitochondrial axis as key regulators of autophagy. *Autophagy* **9**, 1367–1385 (2013).
53. J. Xue, S. Patergnani, C. Giorgi, J. Suarez, K. Goto, A. Bononi, M. Tanji, F. Novelli, S. Pastorino, R. Xu, N. Caroccia, A. U. Dogan, H. I. Pass, M. Tognon, P. Pinton, G. Gaudino, T. W. Mak, M. Carbone, H. Yang, Asbestos induces mesothelial cell transformation via HMGB1-driven autophagy. *Proc. Natl. Acad. Sci. U.S.A.* **117**, 25543–25552 (2020).
54. C. Cardenas, R. A. Miller, I. Smith, T. Bui, J. Molgo, M. Muller, H. Vais, K. H. Cheung, J. Yang, I. Parker, C. B. Thompson, M. J. Birnbaum, K. R. Hallows, J. K. Foskett, Essential regulation of cell bioenergetics by constitutive $InsP_3$ receptor Ca^{2+} transfer to mitochondria. *Cell* **142**, 270–283 (2010).
55. S. Patergnani, P. Pinton, Mitophagy and mitochondrial balance. *Methods Mol. Biol.* **1241**, 181–194 (2015).
56. D. Abreu, F. Urano, Current landscape of treatments for Wolfram syndrome. *Trends Pharmacol. Sci.* **40**, 711–714 (2019).
57. B. Delprat, L. Crouzier, T. P. Su, T. Maurice, At the crossing of er stress and mams: A key role of sigma-1 receptor? *Adv. Exp. Med. Biol.* **1131**, 699–718 (2020).
58. C. Giorgi, S. Marchi, P. Pinton, The machineries, regulation and cellular functions of mitochondrial calcium. *Nat. Rev. Mol. Cell Biol.* **19**, 713–730 (2018).
59. M. Peeters, P. Romieu, T. Maurice, T. P. Su, J. M. Maloteaux, E. Hermans, Involvement of the sigma$_1$ receptor in the modulation of dopaminergic transmission by amantadine. *Eur. J. Neurosci.* **19**, 2212–2220 (2004).
60. M. Bonora, S. Patergnani, A. Rimessi, E. De Marchi, J. M. Suski, A. Bononi, C. Giorgi, S. Marchi, S. Missiroli, F. Poletti, M. R. Wieckowski, P. Pinton, ATP synthesis and storage. *Purinergic Signal* **8**, 343–357 (2012).
61. S. Patergnani, F. Baldassari, E. De Marchi, A. Karkucinska-Wieckowska, M. R. Wieckowski, P. Pinton, Methods to monitor and compare mitochondrial and glycolytic ATP production. *Methods Enzymol.* **542**, 313–332 (2014).
62. C. Giorgi, A. Danese, S. Missiroli, S. Patergnani, P. Pinton, Calcium dynamics as a machine for decoding signals. *Trends Cell Biol.* **28**, 258–273 (2018).
63. E. Pchitskaya, E. Popugaeva, I. Bezprozvanny, Calcium signaling and molecular mechanisms underlying neurodegenerative diseases. *Cell Calcium* **70**, 87–94 (2018).
64. E. L. Wilson, E. Metzakopian, ER-mitochondria contact sites in neurodegeneration: Genetic screening approaches to investigate novel disease mechanisms. *Cell Death Differ.* **28**, 1804–1821 (2021).
65. K. S. Lee, S. Huh, S. Lee, Z. Wu, A. K. Kim, H. Y. Kang, B. Lu, Altered ER-mitochondria contact impacts mitochondria calcium homeostasis and contributes to neurodegeneration in vivo in disease models. *Proc. Natl. Acad. Sci. U.S.A.* **115**, E8844–E8853 (2018).
66. M. Geva, R. Kusko, H. Soares, K. D. Fowler, T. Birnberg, S. Barash, A. M. Wagner, T. Fine, A. Lysaght, B. Weiner, Y. Cha, S. Kolitz, F. Towfic, A. Orbach, R. Laufer, B. Zeskind, I. Grossman, M. R. Hayden, Pridopidine activates neuroprotective pathways impaired in huntington disease. *Hum. Mol. Genet.* **25**, 3975–3987 (2016).
67. D. A. Ryskamp, V. Zhemkov, I. Bezprozvanny, Mutational analysis of sigma-1 receptor's role in synaptic stability. *Front. Neurosci.* **13**, 1012 (2019).
68. H. R. Schmidt, A. C. Kruse, The molecular function of σ receptors: Past, present, and future. *Trends Pharmacol. Sci.* **40**, 636–654 (2019).
69. V. Zhemkov, J. A. Ditlev, W. R. Lee, M. Wilson, J. Liou, M. K. Rosen, I. Bezprozvanny, The role of sigma 1 receptor in organization of endoplasmic reticulum signaling microdomains. *eLife* **10**, e65192 (2021).
70. D. O. Sambo, J. J. Lebowitz, H. Khoshbouei, The sigma-1 receptor as a regulator of dopamine neurotransmission: A potential therapeutic target for methamphetamine addiction. *Pharmacol. Ther.* **186**, 152–167 (2018).

71. V. Matto, A. Terasmaa, E. Vasar, S. Koks, Impaired striatal dopamine output of homozygous Wfs1 mutant mice in response to [K^+] challenge. *J. Physiol. Biochem.* **67**, 53–60 (2011).
72. T. Visnapuu, M. Plaas, R. Reimets, S. Raud, A. Terasmaa, S. Koks, S. Sutt, H. Luuk, C. A. Hundahl, K. L. Eskla, A. Altpere, A. Alttoa, J. Harro, E. Vasar, Evidence for impaired function of dopaminergic system in Wfs1-deficient mice. *Behav. Brain Res.* **244**, 90–99 (2013).
73. T. D. Irons, P. E. Kelly, D. L. Hunter, R. C. Macphail, S. Padilla, Acute administration of dopaminergic drugs has differential effects on locomotion in larval zebrafish. *Pharmacol. Biochem. Behav.* **103**, 792–813 (2013).
74. C. Giorgi, E. Bouhamida, A. Danese, M. Previati, P. Pinton, S. Patergnani, Relevance of autophagy and mitophagy dynamics and markers in neurodegenerative diseases. *Biomedicine* **9**, 149 (2021).
75. L. Cao, M. P. Walker, N. K. Vaidya, M. Fu, S. Kumar, A. Kumar, Cocaine-mediated autophagy in astrocytes involves sigma 1 receptor, PI3K, mTOR, Atg5/7, beclin-1 and induces type II programed cell death. *Mol. Neurobiol.* **53**, 4417–4430 (2016).
76. M. G. Christ, H. Huesmann, H. Nagel, A. Kern, C. Behl, Sigma-1 receptor activation induces autophagy and increases proteostasis capacity in vitro and in vivo. *Cell* **8**, 211 (2019).
77. T. D. MacVicar, L. V. Mannack, R. M. Lees, J. D. Lane, Targeted siRNA screens identify ER-to-mitochondrial calcium exchange in autophagy and mitophagy responses in RPE1 cells. *Int. J. Mol. Sci.* **16**, 13356–13380 (2015).
78. H. Yang, H. Shen, J. Li, L. W. Guo, SIGMAR1/Sigma-1 receptor ablation impairs autophagosome clearance. *Autophagy* **15**, 1539–1557 (2019).
79. T. Kato, M. Ishiwata, K. Yamada, T. Kasahara, C. Kakiuchi, K. Iwamoto, K. Kawamura, H. Ishihara, Y. Oka, Behavioral and gene expression analyses of Wfs1 knockout mice as a possible animal model of mood disorder. *Neurosci. Res.* **61**, 143–158 (2008).
80. M. Plaas, K. Seppa, R. Reimets, T. Jagomae, M. Toots, T. Koppel, T. Vallisoo, M. Nigul, I. Heinla, R. Meier, A. Kaasik, A. Piirsoo, M. A. Hickey, A. Terasmaa, E. Vasar, Wfs1-deficient rats develop primary symptoms of Wolfram syndrome: Insulin-dependent diabetes, optic nerve atrophy and medullary degeneration. *Sci. Rep.* **7**, 10220 (2017).
81. K. Koido, S. Koks, T. Nikopensius, E. Maron, S. Altmae, E. Heinaste, K. Vabrit, V. Tammekivi, P. Hallast, A. Kurg, J. Shlik, V. Vasar, A. Metspalu, E. Vasar, Polymorphisms in wolframin (WFS1) gene are possibly related to increased risk for mood disorders. *Int. J. Neuropsychopharmacol.* **8**, 235–244 (2005).
82. T. Maurice, T. P. Su, A. Privat, Sigma$_1$ (σ_1) receptor agonists and neurosteroids attenuate $\beta_{25\text{-}35}$-amyloid peptide-induced amnesia in mice through a common mechanism. *Neuroscience* **83**, 413–428 (1998).
83. A. Hyrskyluoto, I. Pulli, K. Tornqvist, T. H. Ho, L. Korhonen, D. Lindholm, Sigma-1 receptor agonist PRE084 is protective against mutant huntingtin-induced cell degeneration: Involvement of calpastatin and the NF-κB pathway. *Cell Death Dis.* **4**, e646 (2013).
84. M. Peviani, E. Salvaneschi, L. Bontempi, A. Petese, A. Manzo, D. Rossi, M. Salmona, S. Collina, P. Bigini, D. Curti, Neuroprotective effects of the sigma-1 receptor (S1R) agonist PRE-084, in a mouse model of motor neuron disease not linked to SOD1 mutation. *Neurobiol. Dis.* **62**, 218–232 (2014).
85. N. Sestakova, A. Puzserova, M. Kluknavsky, I. Bernatova, Determination of motor activity and anxiety-related behaviour in rodents: Methodological aspects and role of nitric oxide. *Interdiscip Toxicol* **6**, 126–135 (2013).
86. R. M. Basnet, D. Zizioli, S. Taweedet, D. Finazzi, M. Memo, Zebrafish larvae as a behavioral model in neuropharmacology. *Biomedicine* **7**, 23 (2019).
87. X. Peng, J. Lin, Y. Zhu, X. Liu, Y. Zhang, Y. Ji, X. Yang, Y. Zhang, N. Guo, Q. Li, Anxiety-related behavioral responses of pentylenetetrazole-treated zebrafish larvae to light-dark transitions. *Pharmacol. Biochem. Behav.* **145**, 55–65 (2016).
88. S. J. Schnorr, P. J. Steenbergen, M. K. Richardson, D. L. Champagne, Measuring thigmotaxis in larval zebrafish. *Behav. Brain Res.* **228**, 367–374 (2012).
89. C. Kilkenny, W. Browne, I. C. Cuthill, M. Emerson, D. G. Altman; N. C. R. R. G. W. Group, Animal research: Reporting in vivo experiments: The ARRIVE guidelines. *Br. J. Pharmacol.* **12**, 561–563 (2010).
90. T. Hayashi, E. Hayashi, M. Fujimoto, H. Sprong, T. P. Su, The lifetime of UDP-galactose:ceramide galactosyltransferase is controlled by a distinct endoplasmic reticulum-associated degradation (ERAD) regulated by sigma-1 receptor chaperones. *J. Biol. Chem.* **287**, 43156–43169 (2012).
91. F. Duclot, M. Lapierre, S. Fritsch, R. White, M. G. Parker, T. Maurice, V. Cavailles, Cognitive impairments in adult mice with constitutive inactivation of RIP140 gene expression. *Genes Brain Behav.* **11**, 69–78 (2012).
92. T. Maurice, F. Duclot, J. Meunier, G. Naert, L. Givalois, J. Meffre, A. Celerier, C. Jacquet, V. Copois, N. Mechti, K. Ozato, C. Gongora, Altered memory capacities and response to stress in p300/CBP-associated factor (PCAF) histone acetylase knockout mice. *Neuropsychopharmacology* **33**, 1584–1602 (2008).
93. M. Bonora, C. Giorgi, A. Bononi, S. Marchi, S. Patergnani, A. Rimessi, R. Rizzuto, P. Pinton, Subcellular calcium measurements in mammalian cells using jellyfish photoprotein aequorin-based probes. *Nat. Protoc.* **8**, 2105–2118 (2013).
94. G. J. Brewer, J. R. Torricelli, Isolation and culture of adult neurons and neurospheres. *Nat. Protoc.* **2**, 1490–1498 (2007).
95. S. Patergnani, M. Bonora, S. Ingusci, M. Previati, S. Marchi, S. Zucchini, M. Perrone, M. R. Wieckowski, M. Castellazzi, M. Pugliatti, C. Giorgi, M. Simonato, P. Pinton, Antipsychotic drugs counteract autophagy and mitophagy in multiple sclerosis. *Proc. Natl. Acad. Sci. U.S.A.* **118**, e2020078118 (2021).
96. F. Tomassoni-Ardori, Z. Hong, G. Fulgenzi, L. Tessarollo, Generation of functional mouse hippocampal neurons. *Bio Protoc* **10**, e3702 (2020).

Acknowledgments: We thank S. Koks for providing the colony founders and G. Lutfalla (LPHI, Montpellier, France) for the PCS2$^+$ mCherry plasmid. This work was a project (#15) of the CompAn behavioral phenotyping facility (Montpellier, France). We thank the ZebraSens behavioral phenotyping platform (MMDN) and the breeding facility from the University of Montpellier (RAM-CECEMA). We thank the animal facility of the Institute of Neurosciences of Montpellier and the Reseau des animaleries de Montpellier (RAM) for help in animal breeding and handling. We also thank A. Peyrel for technical assistance. **Funding:** This work was supported in part by external resources of the University of Montpellier (Fondation Pour l'Audition FPA RD-2019-13, Retina France Association and Foundation to B.D.) and in part by the Intramural Research Program of the National Institute on Drug Abuse/NIH (to T.-P.S.). P.P. is grateful to Camilla degli Scrovegni for continuous support. P.P. is supported by the Italian Association for Cancer Research (AIRC: IG-23670), Associazione Ricerca Oncologica Sperimentale Estense (A-ROSE), Progetti di Rilevante Interesse Nazionale (PRIN2017E5L5P3), and local funds from the University of Ferrara. S.P. is supported by Fondazione Umberto Veronesi. L.C. is supported by Association syndrome de Wolfram and the Région Occitanie and Elodie M. Richard by The Snow Foundation and Eye Hope Foundation. **Author contributions:** B.D., T.M., and T.-P.S. conceived the project and designed the experiments. L.C. performed most of the in vivo experiments and analyses. C.D., M.D., and M.R. performed visual motor response experiments. N.C. took care of the zebrafish. A.D. and S.P. performed in vitro aequorin and Seahorse experiments. Y.Y. and S.C. performed biochemical and histological experiments. A.D., S.P., and P.P. performed in vitro experiments and analyses. J.-C.L. performed zebrafish injections. T.-P.S. provided access to S1R KO and NG-108 cells. B.D. and T.M. performed part of the in vivo mouse experiments, prepared the figures, and wrote the manuscript. E.M.R. implemented the manuscript. All authors contributed to the preparation of the figures and manuscript writing. **Competing interests:** T.M. consulted for Zogenix and Prilenia Therapeutics and holds patents on sigma-1 drugs (Novel phosphinolactone derivatives and pharmaceutical uses thereof, WO2017191034A1; Sigma-1 receptor ligands and uses thereof, EP19306705; Sigma-1 receptor ligands and uses thereof, EP19306706). B.D. and T.M. filed a patent (Sigma-1 receptor activator for use in the treatment of a pathology associated with wfs1 mutation, EP pending 21306072.6). All other authors declare that they have no competing interests. **Data and materials availability:** All data associated with this study are present in the paper or the Supplementary Materials. A material transfer agreement between Karlsruhe Institute of Technology and Inserm ADR Montpellier exists for *wfs1a*^{C799X} and *wfs1b*^{W493X} zebrafish lines.

Submitted 4 March 2021
Resubmitted 21 October 2021
Accepted 17 December 2021
Published 9 February 2022
10.1126/scitranslmed.abh3763

Science Translational Medicine

Activation of the sigma-1 receptor chaperone alleviates symptoms of Wolfram syndrome in preclinical models

Lucie CrouzierAlberto DaneseYuko YasuiElodie M. RichardJean-Charles LiévensSimone PatergnaniSimon CoulyCamille DiezMorgane DenusNicolas CubedoMireille RosselMarc ThiryTsung-Ping SuPaolo PintonTangui MauriceBenjamin Delprat

Sci. Transl. Med., 14 (631), eabh3763.

Treating Wolfram syndrome in the ER

Wolfram syndrome (WS) is a genetic disease characterized by early diabetes, optic atrophy, and deafness caused by mutations in the *WSF1* gene. Pathologic mutations lead to altered communication between the endoplasmic reticulum (ER) and the mitochondria within the mitochondria-associated ER membranes (MAMs), ultimately resulting in impaired mitochondrial function and cell death. Here, Crouzier *et al.* used preclinical models of wolframin deficiency and showed that activation of the sigma-1 receptor in the ER restored MAM alterations, boosted mitochondrial function, and improved behavioral symptoms in zebrafish and rodents. The study identified a potential therapeutic target that could be targeted for alleviating symptoms in patients with WS and other MAM-related diseases.